



0079-6611(95)00013-5

## The climatology of the North Atlantic

M. SUSAN LOZIER<sup>1</sup>, W. BRECHNER OWENS<sup>2</sup> and RUTH G. CURRY<sup>2</sup>

<sup>1</sup>*Ocean Sciences Program, Duke University, Durham, North Carolina, USA*

<sup>2</sup>*Woods Hole Oceanographic Institution, Woods Hole, Massachusetts, USA*

**Abstract** - Data from approximately 144,000 hydrographic stations in the North Atlantic have been retrieved from the national Oceanic Data Centre and analysed to produce maps of mean pressure, temperature, salinity and oxygen on selected potential density surfaces for the domain bounded by 0°-85°W and 0°-65°N. The data span the period from 1904 to 1990 with the majority of the data from the last four decades. The data set for this region is 60% larger than that used in the production of Levitus' Climatological World Atlas. This increase in stations, coupled with smoothing scales specific to the North Atlantic rather than the global ocean, considerably improves the resolution of the basin's features. The mean property fields and their associated standard deviations are resolved on a one-degree grid with little smoothing, contrasting with the Levitus Atlas where properties, although presented on a one-degree grid, have been smoothed on the order of 1000km. Another important feature of this database is the process by which irregularly spaced data are averaged onto a regular grid. In a significant departure from the Levitus analysis, which averaged on depth surfaces, these data were averaged on potential density surfaces, thus eliminating an artificial mixing of water mass properties. The database is used to describe the baroclinicity of well-known features such as the Gulf Stream, the North Atlantic Current and the Deep Western Boundary Current, and to elucidate the recirculations associated with these currents. It additionally resolves several new features in the intermediate and deep North Atlantic. These features include the signature of a large scale deep recirculation that extends southwestward from the eastward extension of the North Atlantic Current to the separation point of the Gulf Stream near Cape Hatteras. This recirculation, which spans approximately 2000m of the water column, encompasses more local recirculations and potentially mixes subpolar and subtropical waters. Furthermore, in the upper thermocline, this database reveals a coherent Azores Current that stretches from the Gulf Stream system south of the Tail of the Grand Banks to Madeira. This flow is marked by divergences to the south and convergences from the north such that its downstream transport is not much changed.

## CONTENTS

1.	Introduction	2
2.	Data sources and distribution	3
3.	Quality control	7
3.1	Range checking	7
3.2	Statistical checking	8
3.3	Oxygen quality	9
3.4	Data biases	10
4.	Data presentation	10
4.1	Selected potential density surfaces	11
4.2	Averaging and smoothing	11
5.	Property fields	13
5.1	$\sigma_0 = 26.50$	14
5.2	$\sigma_0 = 27.00$	19
5.3	$\sigma_1 = 31.85$	23
5.4	$\sigma_1 = 32.35$	26
5.5	$\sigma_2 = 36.95$	29
5.6	$\sigma_3 = 41.45$ and $41.50$	32
5.7	$\sigma_4 = 45.90$	36
6.	Comparison with Levitus fields	39
7.	Summary	41
8.	Acknowledgements	42
9.	References	42

## 1. INTRODUCTION

During the past century numerous hydrographic studies of the North Atlantic have yielded synoptic descriptions of this ocean basin. Particularly notable are the atlases of WÜST and DEFANT (1936), FUGLISTER (1960), and WORTHINGTON and WRIGHT (1970). In 1982, the publication of the *Climatological Atlas of the World Ocean* (LEVITUS, 1982) provided a climatological description of the hydrographic fields of the global ocean. Because of its quality and availability, this atlas, which has recently been updated (LEVITUS, 1994) to include more recent data, has become a standard as well as an invaluable resource to the oceanographic community. Although Levitus' atlas can serve many needs, increases in computational efficiency have fueled a demand for climatology with finer resolution. As scientists in the 1990s focus their efforts on quantifying the role of the oceans in the global climate system and numerical models of ocean circulation are able to economically resolve ever smaller scales of motion, databases and analytical tools must evolve to match their needs. Our motivation in producing a climatological atlas specific to the North Atlantic is based on the general recognition that the North Atlantic, with its active deep water formation sites, plays a crucial role in the climate of the global ocean. Key to evaluating climatic variability is a determination of the North Atlantic's *mean* water mass properties and circulations. These efforts require more highly resolved climatological fields than those currently available. The global scope of the Levitus atlas is reflected in its uniformly smoothed, but coarsely resolved, property fields where each one-degree gridpoint is smoothed using selected influence radii the smallest of which is 771 km. In the preparation of a database specific to the data-rich North Atlantic we were able to considerably decrease the smoothing of the property fields to scales of 100-300 km. This goal was aided by a 60% increase in available station data in the North Atlantic since Levitus assembled his original database.

In a distinct departure from the Levitus work, we chose to analyse the data on potential density surfaces rather than on depth surfaces. Because there is widespread acceptance of the dominance

of isopycnal mixing over diapycnal mixing, we believe that averaging on isopycnals more closely mimics real ocean processes. Supporting this supposition is the recent work by LOZIER, MCCARTNEY and OWENS (1994) which demonstrates that isobaric averaging in the vicinity of sloping isopycnals produces average water properties that are dissimilar to the *in situ* water masses. This work further shows that such artifacts are avoided with isopycnal averaging. Another advantage of isopycnal averaging is that in many regions, including the vicinity of the Gulf Stream, spatial property gradients are smaller on isopycnals than on isobars, thus reducing the effect of spatial smoothing along a surface.

In summary, our work parallels Levitus' effort in that we have compiled a three-dimensional climatology of the North Atlantic basin based on all available historical station data. However, our analysis differs primarily in its use of isopycnal averaging and smaller smoothing scales. This paper outlines our efforts in the preparation of this hydrographic database and represents the climatological means for temperature, salinity, pressure and oxygen on selected potential density surfaces. The selection is intended to demonstrate the fields from a number of water mass and circulation regimes, without being all-encompassing in either the selection or the discussion of the surfaces. The data sources and distribution are discussed in section 2, the quality control of the data are discussed in section 3 and the averaging and smoothing are discussed in section 4. The property fields are presented in section 5, followed by a comparative study with Levitus fields in section 6 and a summary in section 7. A basemap of the geographic and topographic features referred to in the text is given in Fig. 1.

## 2. DATA SOURCES AND DISTRIBUTION

The 143,879 original stations used in this synthesis were obtained from the National Oceanographic Data Centre (NODC) and represent all hydrographic station data available as of April 1990 for the geographic domain bounded by 0° to 75°N and 85° to 20°E. Our quality control reduced the final number of stations by approximately 9%, to a total of 131,635. The horizontal, vertical and temporal distributions of the data, to be presented next, are based on this number of stations.

The horizontal distribution of stations used in this analysis is shown in Fig. 2. The greatest density of stations occurs along the western boundary of the basin, particularly in the vicinity of the Gulf Stream and the frontal mixing zones around the Grand Banks. Sparser sampling (<10 stations per 1-degree square) predominates in the relatively quiescent gyre interior. Such sampling biases predictably result from several factors: (1) scientific interest in frontal areas; (2) the number of data points needed to adequately describe a region (which is proportional to its variability); and (3) proximity to land and/or ports of call. High station densities also coincide with weather ship locations and occasional intensive eddy experiments. Although an ideal situation would provide equal and dense sampling everywhere in the ocean, the actual distribution does not greatly compromise our ability to produce statistically meaningful information. It does, however, dictate the scales at which the data should be analysed. Ideally, the unit area over which averages are computed should be small enough so that the stations within it possess uniform water mass properties, yet large enough so that a sufficient number of data points contribute to the evaluation of the property means. Fortunately, the tendency towards dense sampling in frontal zones permits us to compute mean properties for small unit areas (1-degree square) in these locales, thus preserving the structure and intensity of the regional property gradients. Conversely, the sparser sampling of the gyre interior forces us to average over larger geographic areas (3-degree square) to attain a sufficient number of data points.

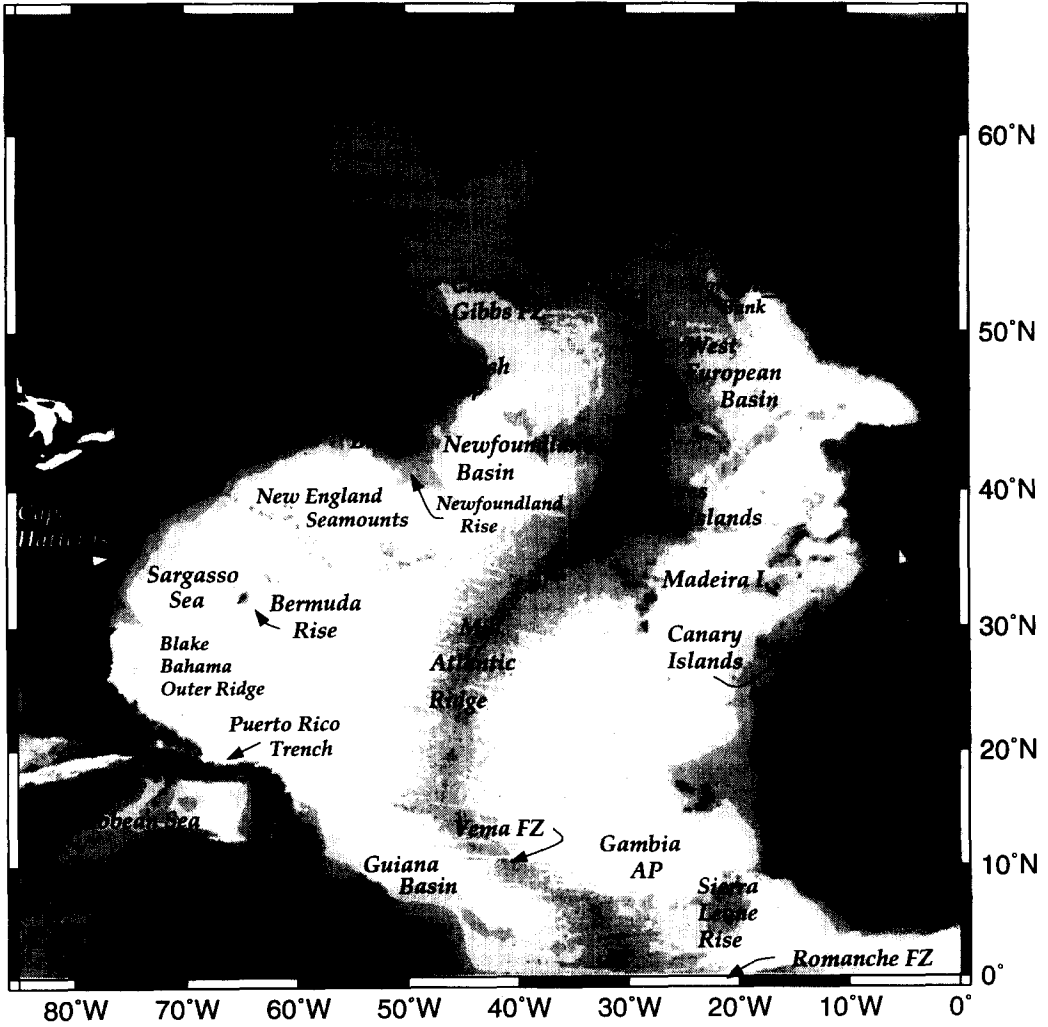


Fig.1. Topographic and geographic features referred to in the text.

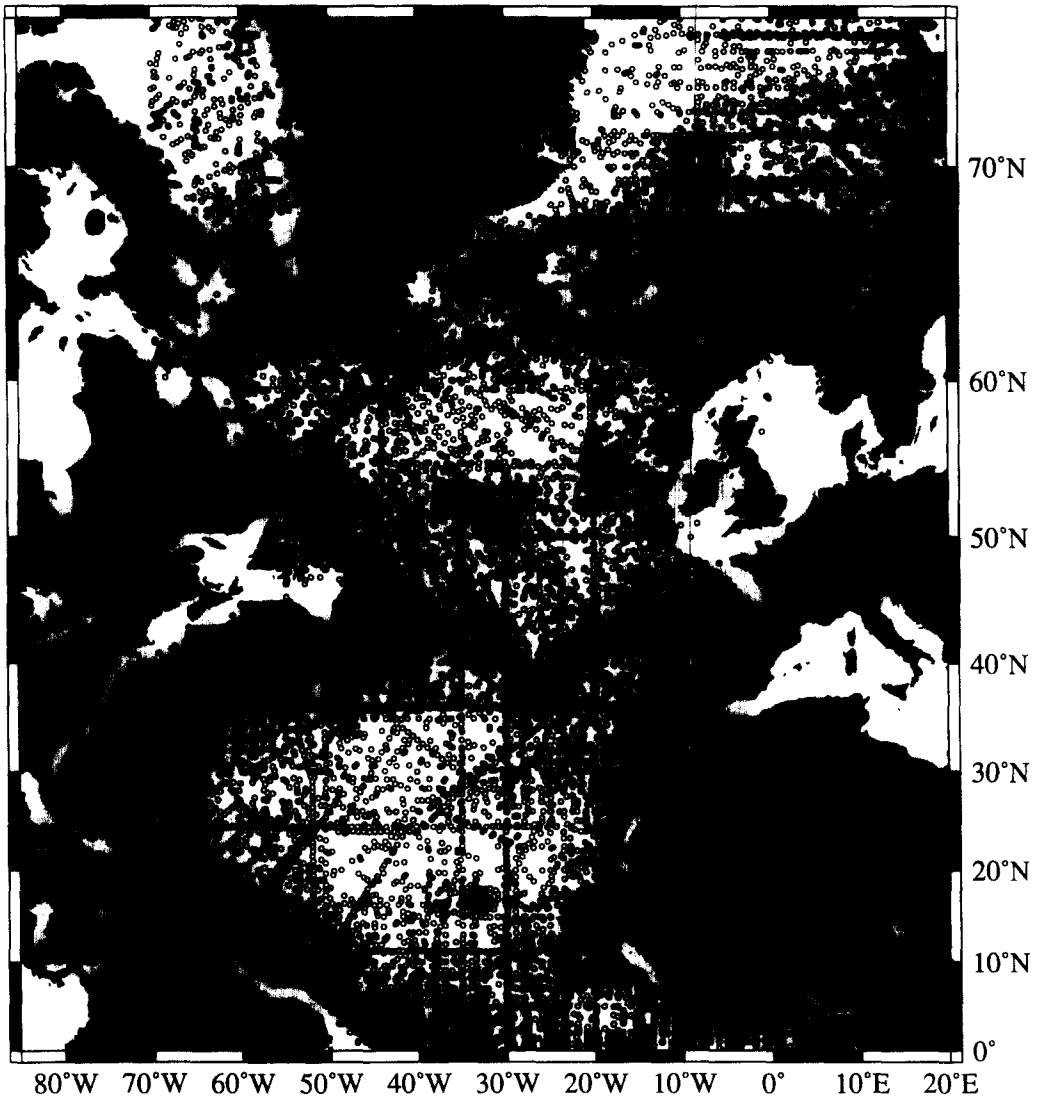


Fig.2. Location of hydrographic stations used in the preparation of this database. Only those stations which met our quality control standards are depicted. Total number of stations is 131,635.

In addition to horizontal inhomogeneities, the sample distribution also lacks vertical consistency. The number of samples decreases substantially with increasing depth, as shown in Fig.3. Above 200m, more than 90% of stations contain at least one temperature/salinity observation in each of the ranges bounded by the NODC oceanographic standard depths (LEVITUS, 1982). That number drops to 80% near 500m, oscillates between 50-70% down to 1500m, then declines precipitously to less than 20% below 2500m. The percentage of oxygen samples, though more consistent throughout the water column, falls everywhere below 30% of potential sample numbers and drops off to less than 10% below 2500m.

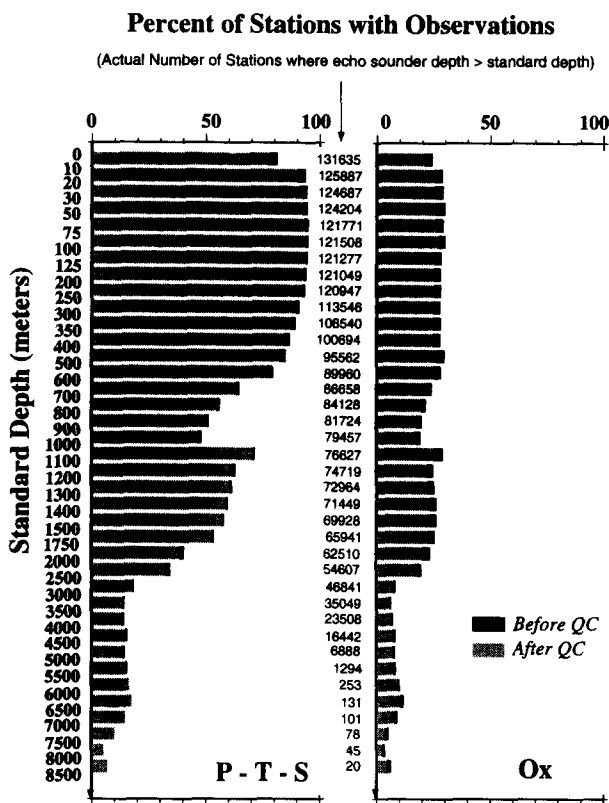


Fig.3. Vertical distribution of observations. Each bar depicts the percentage of stations in which at least one observation was made between the standard depths listed on the y-axis. This percentage is based only on the number of stations where the sea floor is deeper than the standard depth.

The station data are temporally distributed between the years 1904 and 1990, with the bulk of the data collected since the late 1950s (Fig.4). Data density peaks in the early 1970s, followed by a gradual decline until the mid-1980s. The sharp drop in available data collected after 1985 reflects the accumulated lag between data collection, submission to NODC and data entry into the archives. The property fields presented here represent means and associated standard deviations computed for the entire temporal span of station data.

## Temporal Distribution of Stations

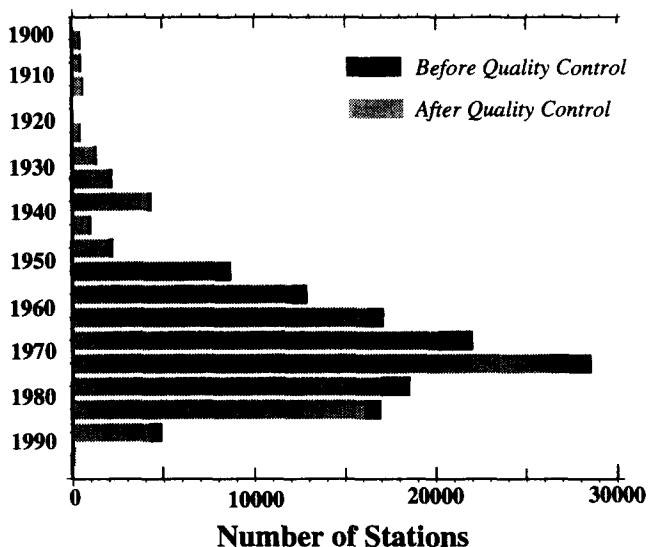


Fig.4. Temporal distribution of the station data. Each bar spans a five-year time period.

### 3. QUALITY CONTROL

Since producing a database representative of the mean state of the North Atlantic basin was the central goal of this work, our quality control methods were designed to identify and eliminate erroneous data and data that are clearly atypical for a given locale. To meet this goal the observations were subjected to three quality control steps that are detailed in this section: (1) a range check, (2) a statistical check for the identification of outliers, and (3) a visual review of variance plots for each property. Collectively, these steps reduced the number of stations by 8.5%. Before applying this set of checks, we eliminated a subset of stations which geographically did not belong in this synthesis: coastal areas (<200m deep), the Mediterranean Sea, the North Sea, the Gulf of St Lawrence, and the Gulf of Maine. We intend to restore the shelf areas, which comprise an additional 250,000 stations, to the database at a later date.

#### 3.1 Range checking

A preliminary check of the data eliminated values that were outside of broad property ranges. These ranges (for temperature, salinity and oxygen) were defined as a function of depth and latitude using atlases and synoptic sections of the North Atlantic for guidance. This range check eliminated 375 temperatures, 20,933 salinities and 1 oxygen value. The majority of bad salinity values came from a series of USSR cruises. Levitus similarly reported a large number of spurious USSR salinity values in his quality control checks. Although he chose to eliminate all USSR salinity values below 400m, we opted against such a blanket exclusion, relying instead upon the statistical check to identify questionable data. Because subsequent quality control steps would require the ability to

compute potential density, any observation level missing either temperature or salinity was entirely eliminated. Temperature and salinity were retained for any level missing only an oxygen value. A total of 1268 stations (0.9%) were eliminated because they lacked either temperature or salinity observations at all levels.

### 3.2 Statistical checking

In order to further identify questionable data points, we used the fact that potential temperature-salinity ( $\theta$ -S) and potential temperature-oxygen ( $\theta$ -O<sub>2</sub>) relationships are locally well-defined for the North Atlantic. Plots of  $\theta$ -S and  $\theta$ -O<sub>2</sub> for all stations within a discrete geographic area illustrate these relationships and graphically reveal data points that deviate significantly from them. These plots are often used to visually identify erroneous points from data as it is collected and analysed. Because hand-picking outliers from visual representations of 140,000 stations was obviously not a viable option, outliers were instead identified by a series of computations detailed below.

We first subdivided the data into geographic areas to achieve a balance between two goals: (1) to create groups with similar  $\theta$ -S and  $\theta$ -O<sub>2</sub> profiles; and (2) to have sufficient stations in each group in order to establish statistically significant mean property relations. Using all station data within a 5-degree square area,  $\theta$ -S and  $\theta$ -O<sub>2</sub> plots were created. In areas which showed a large degree of scatter in the property relationships, 2.5-degree subdivisions were made. If that subdivision was inadequate to obtain relatively tight property-property relationships the data were further subdivided into 1-degree squares. Where the station density was low, we combined neighbouring 1-degree squares into larger areas to achieve a minimum of ten stations per area. Figure 5 shows these geographic subdivisions.

The  $\theta$ -S curve for each geographic subdivision was approximated by subdividing the observed points into vertically contiguous density bins for which the mean  $\theta$ -S and  $\theta$ -O<sub>2</sub> relations were approximately linear. The density bins, specific to geographic locale, were chosen empirically by superimposing isopycnals onto the  $\theta$ -S diagrams and then increasing the number of density bins until the line segments closely approximated the shape of the  $\theta$ -S curve. The mean ( $\theta$ ,S) points in each density bin were connected and the line tangent to this curve at its mean ( $\theta$ ,S) was used to approximate the  $\theta$ -S relation for a bin (Fig.6). The standard deviation of salinity observations as a function of potential temperature was then computed for each density bin. Although density varies mainly as a function of potential temperature, in some locations, most notably the subpolar region and the sea surface, salinity has a larger influence. In these instances, where the slope of the  $\theta$ -S curve exceeded 1.0psu/°C, salinity was used as the independent parameter in evaluating the standard deviation. For each observed  $\theta$  (or S), the distance from the tangent line to its corresponding S (or  $\theta$ ) observation determined if the point was acceptable. We defined an acceptable range of observations by a distance of  $\pm 2.3$  standard deviations from the tangent line; points falling outside this envelope were eliminated. This limit was chosen on the statistical basis that approximately 98% of all observations in a normally distributed population will fall within 2.3 standard deviations on either side of the mean (KREYSZIG, 1979). If a  $\theta$ -S pair fell outside this envelope the entire scan was eliminated because we would later need both properties to compute density. Additionally, any point, whose density fell into none of the defined bins or into a bin containing less than three points, was eliminated. Finally, any station having greater than 20% bad observations was completely eliminated. Similar characterizations were made for the  $\theta$ -O<sub>2</sub> (or S-O<sub>2</sub>) relation, where the standard deviation of oxygen observations was computed as a function of potential temperature (or salinity when it varies more rapidly than potential temperature). Any oxygen point which fell outside of the allowable range ( $\pm 2.3$  standard deviations) was eliminated, but the temperature and salinity observations were retained.

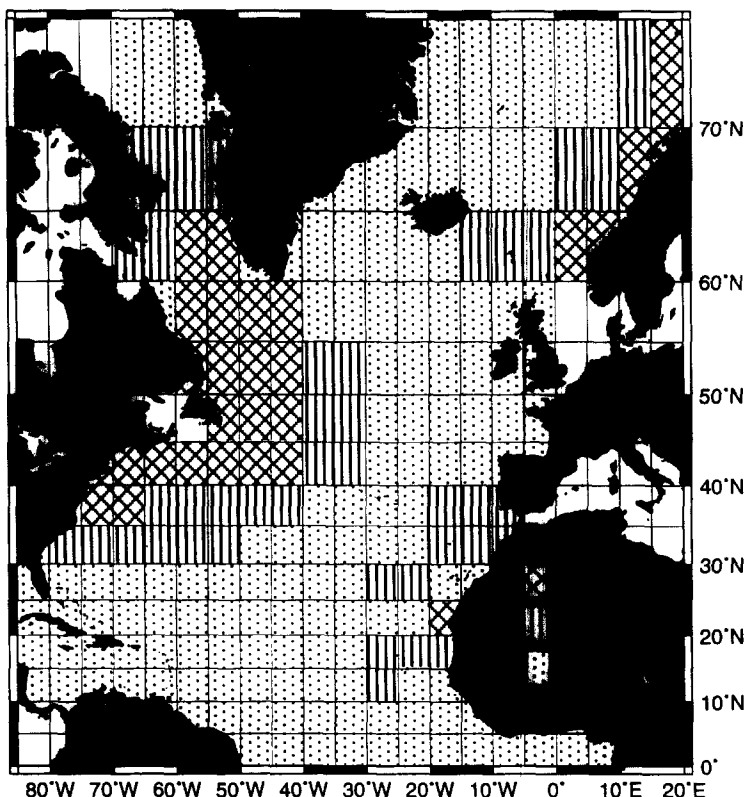


Fig.5. Geographic subdivisions implemented in our quality control. The 1°, 2.5°, or 5° square areas were assigned on the basis of uniformity of  $\theta$ -S characteristics.

This statistical procedure was applied twice to the database. The first pass eliminated 7792 stations (5.5%). Temperature/salinity (oxygen) outliers were identified in 6.6% (12.7%) of the individual scans. The higher oxygen elimination reflects the removal of even a good oxygen point if its associated temperature or salinity failed the test. For the second pass, the data which emerged from the first check were used to recompute the means and standard deviations for the property relations. An additional 1760 stations (1.3%) were eliminated. For this pass, temperature/salinity (oxygen) outliers were identified in 2.3% (4.58%) of the individual scans. Overall, the statistical check reduced the database by 6.6%, to a total of 132,608 stations. Finally, we note that this data elimination was distributed uniformly over the water column; Fig.3 shows that the vertical distribution of observations is virtually identical before and after this procedure.

### 3.3 Oxygen quality

The method for titrating oxygen samples changed in the late 1950s from a potassium dichromate standard to a bi-iodate standard. Although WORTHINGTON (1976) suggested multiplying all data produced with the old standard by 1.048 to agree with the modern data, this factor is based solely on data obtained from Woods Hole cruises. Because of this problem, and other potential inconsistencies with the pre-1960 methods, we have reluctantly opted to eliminate older oxygen data (pre-1960) completely from the database rather than attempt to adjust those values.

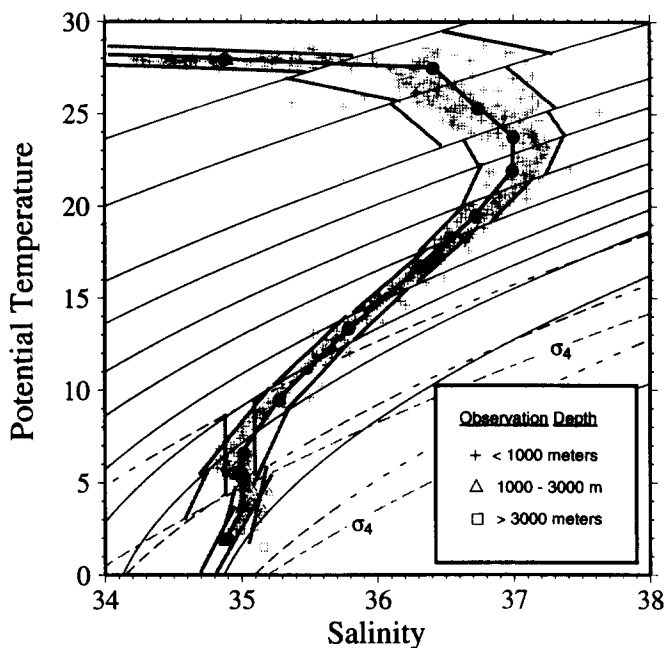


Fig.6. A  $\theta$ -S diagram from actual observations in a  $5^\circ$  square area. The fitted  $\theta$ -S curve (solid center line) is shown with filled symbols marking the mean  $\theta$ -S pairs for each density bin. The broken line segments define the 2.3 standard deviation envelope for each bin. Those points outside of this envelope were eliminated from our database. The contours delineate the sigma bins used to vertically subdivide the data. Sigma-0 contours are solid, sigma-2 contours are dashed, and sigma-4 contours are both dashed and labelled. Three different symbols represent the depth ranges of each observation, as indicated in the inset box.

### 3.4 Data biases

Peculiarities in the property fields calculated from this data set illuminated a few additional problems which had slipped through our quality control net. Contoured fields of the standard deviations for each property proved a useful tool in identifying some remaining questionable values. In several instances, data from a single cruise with many stations adversely biased the mean in a particular area. This manifested itself as a strong local feature (a “bull’s eye”) in the standard deviation field. In these cases, we removed the suspect cruise from the original set of stations, and completely recomputed the statistical check for that area. For purposes of comparison to our quality-controlled database, an unedited version of the original data file is maintained online.

## 4. DATA PRESENTATION

Using this quality-controlled, yet unevenly distributed set of station data, our next goal was to create a 1-degree gridded data set of mean properties on potential density surfaces. The selection of surfaces and the methods of averaging and smoothing the data are detailed in this section. At this point we make a distinction between the hydrographic *database*, which consists of the quality controlled station data, and *adata set*, which consists of gridded and smoothed data projected onto

selected surfaces. The latter is a product of the former. To maximize the utility of our database, we have developed a set of software tools that allows a user to create any number of data sets from the primary database. For a desired application a user may select, for example, the gridding interval, the smoothing scales and the surfaces for projection. Our interest in delineating basin scale features dictated the parameter choices for this study.

#### 4.1 Selected potential density surfaces

The property distribution on a given potential density surface can be created from the hydrographic database we have produced. For our analysis we selected a dozen density surfaces spanning the water column. However, for the purpose of this paper we present the fields from eight representative potential density ( $\sigma$ ) surfaces which have the following approximate pressure (P), potential temperature ( $\theta$ ) and salinity (S) ranges:

$\sigma_0 = 26.50$	P: 0 to 400db	$\theta$ : 0 to 18°C	S: 33.0 to 36.6
$\sigma_0 = 27.00$	P: 0 to 700db	$\theta$ : 0 to 13.4°C	S: 33.2 to 36.0
$\sigma_1 = 31.85$	P: 0 to 900db	$\theta$ : 0 to 12°C	S: 33.6 to 36.0
$\sigma_1 = 32.35$	P: 400 to 1600db	$\theta$ : 3.4 to 12°C	S: 34.8 to 37.5
$\sigma_2 = 36.95$	P: 1400 to 2400db	$\theta$ : 3.2 to 5°C	S: 34.94 to 35.5
$\sigma_3 = 41.45$	P: 1500 to 3100db	$\theta$ : 2.7 to 3.3°C	S: 34.93 to 35.1
$\sigma_3 = 41.50$	P: 2000 to 3600db	$\theta$ : 2.3 to 2.7°C	S: 34.92 to 35.0
$\sigma_4 = 45.90$	P: 3000 to 5000db	$\theta$ : 1.74 to 2.0°C	S: 34.87 to 34.93

(The subscript for potential density indicates the reference level, in db/1000.) These density surfaces were chosen on the basis of their representativeness in terms of water mass properties and major circulation features of the North Atlantic. This choice of surfaces is subjective and we do not claim to have captured the minimum number of surfaces required to describe the vertical structure of the ocean's property fields. We also note here that the choice of a single reference level for these isopycnals leads in some cases (particularly at depth) to isopycnal depths several hundreds of meters away from the reference level. To test the effect of this deviation, fields computed using various reference levels were compared. For example, the temperature field for  $\sigma_4 = 45.90$  was compared to the temperature field for  $\sigma_3 = 41.55$  in the northern part of our domain where the 45.90 isopycnal surface ascends to 3000db. (41.55 is the potential density equivalent to 45.90, using a reference level of 3000db.) For the purpose of the qualitative analyses in this paper we found the differences to be minimal over the domain we studied. However, we recognise that for other applications the differences may be significant. Thus, a user of this database may select reference levels appropriate for their application, they may want to introduce the use of multiple reference levels for a single isopycnal (REID, 1994) or they may chose to compute neutral surfaces using the database (McDOUGALL, 1987).

Finally, we note that although our database extends geographically to 75°N and 20°E, the maps presented here are bounded by 0° - 65°N and 0°-85°W. The suite of density surfaces which represent the North Atlantic are not appropriate to describe the circulation in Baffin Bay, or the Icelandic and Norwegian Seas because the waters within these regions are so dense.

#### 4.2 Averaging and smoothing

The averages which comprise this data set were constructed in an Eulerian framework, common to most numerical and inverse models. Although this broadens and smooths the appearance of

temporally meandering currents such as the Gulf Stream, we are concerned here with placing all currents and property fronts of the North Atlantic in their true geographic context. Other techniques, such as stream coordinate averaging, could generate a description closer to that of the instantaneous Gulf Stream by repositioning the station data with respect to the Gulf Stream, but this would require ancillary synoptic information on the shape and position of the Gulf Stream. Such a restriction would severely curtail the amount of data which could be used for our computations. Furthermore, one would also have to include the statistics of the position of the streamwise coordinates to complete this description.

A gridded matrix in which each gridpoint was centered on a one-degree square was established for the geographic domain. For each station the data were linearly interpolated to project a property value onto a set of potential density surfaces. To avoid situations where interpolation over large vertical distances would generate significantly erroneous property values, limits over which a vertical interpolation would be made were set at 200m in the upper 1000m of the water column; for greater depths the limit was increased to 1000m. If the vertical resolution around the projection surface failed to satisfy these limits, no information from the station was incorporated into the averages for that projection surface. This approach differs from LEVITUS (1982, 1994) where every station profile is interpolated, often over large vertical gaps where the bottle data were either missing or thrown out for quality reasons. Additionally, contrary to the Levitus dataset, where the deepest observation at each station is lost unless it happens to coincide with a standard depth, our interpolation onto selected density surfaces preserves the deepest observation, improving the resolution on the densest surfaces. Finally, every observation within a 1-degree square received equal weighting regardless of its distance from the gridpoint. The mean value, standard deviation, and number of observations for each property were computed.

Each matrix of averaged values representing a surface was smoothed in a three-part process consisting of two low-pass filters and an interpolation procedure. The smoothing algorithms we chose were appropriate to this application, however, to accommodate other applications of this database the three steps remain decoupled so that each can be tuned or substituted by other methods. The first smoothing step implemented a low-pass filter based on the density of observations per gridpoint. The sampling at each point in our gridded matrices varied widely from having hundreds of stations to having no stations. A minimum of ten observations was chosen to adequately define a mean property value at each gridpoint. Statistically, this number of observations guarantees us 90% confidence that a computed mean will fall within one half of a standard deviation from the true mean for a normal distribution of values (KREYSZIG, 1979). If a gridpoint was defined by an ample number of observations, it was not additionally smoothed in this procedure. Conversely, where only a few or no observations defined a gridpoint, information from a larger area was incorporated to define the mean property values. We note again that the station distribution map shows that station density is not random. The highest station densities are clustered near-shore and around the Gulf Stream while the lowest station densities predominate in the gyre interior. Therefore this algorithm will, in general, smooth the interior of the North Atlantic and deeper surfaces more than the coastal (off-shelf) or frontal regions, and shallower surfaces. If less than a total of ten observations contributed to the 1-degree average at any gridpoint in a matrix, information from all squares lying one gridpoint (1-degree) further away was incorporated to produce a 3-degree smoothed value. Each additional point was weighted not only by its number of observations, but also by a distance factor equal to  $1/4d$ , where  $d$  is the number of squares away from the gridpoint being computed. For this presentation of the North Atlantic, no smoothing was performed beyond 3 degrees.

A second type of low-pass filter was next applied to the matrix to reduce variability on the scale of the gridpoint spacing. This spatial filtering was a necessary preprocessing step prior to producing the contours, and amounted to a simple 2-degree block average of the area surrounding each grid-point. Block averages using larger areas (3, 4-degree etc.) produced noticeably smoother contours, but at the expense of the resolution of the property gradients. The third stage of the smoothing, used for producing the contour plots presented below, was accomplished using continuous curvature splines under tension, a method developed by SMITH and WESSEL (1990), who coded the algorithm and distributed it with their GMT graphics software (WESSEL and SMITH, 1991). The method fits a surface with continuous second derivatives and minimal curvature to the matrix of already gridded data, interpolating where necessary to fill holes in the gridded mesh. Adding tension to the solution avoids the large oscillations and extraneous inflection points which are a frequent side effect of the natural bicubic spline interpolant. All property fields presented here were fitted by this method using an interior tension factor of 0.5 and a boundary tension of 0.0 on an overall scale ranging from 0 to 1 (SMITH and WESSEL, 1990).

## 5. PROPERTY FIELDS

The distribution of potential temperature, salinity and oxygen are used to characterize the water masses on each selected potential density surface. Additionally, pressure on each isopycnal is shown to establish the topography of the surface and to give an indication of vertical shear. More commonly, vertical shear is depicted with maps of density on constant depth or pressure surfaces. In such a case the thermal wind relations give a direct proportionality between the shear and the horizontal density gradient:

$$\partial(\rho f v) / \partial z = -g(\partial \rho / \partial x)_z \quad (1a)$$

and

$$\partial(\rho f u) / \partial z = g(\partial \rho / \partial y)_z, \quad (1b)$$

where the subscript is used to denote differentiation along a surface of constant depth. A transformation of these relations to an isopycnal coordinate system yields:

$$\partial(\rho f v) / \partial z = g \partial \rho / \partial z (\partial z / \partial x)_\rho \quad (2a)$$

and

$$\partial(\rho f u) / \partial z = -g \partial \rho / \partial z (\partial z / \partial y)_\rho \quad (2b)$$

In this case, vertical shear is proportional to the slope of the isopycnal times the local vertical density gradient. Because the horizontal pressure gradient on an isopycnal is essentially equivalent to the slope of an isopycnal, a pressure map yields the direction of the vertical shear, with the spacing proportional to its intensity, if the vertical density gradient were constant on that surface.

MONTGOMERY (1937) defined the horizontal geostrophic flow on a surface of constant specific volume anomaly ( $\delta$ ) in terms of a streamfunction,  $\psi_M$ , (where  $\nabla\psi_M = \mathbf{k} \times \mathbf{fu}$ ), given by:

$$\psi_{M,a} - \psi_{M,r} = \delta_a P_a - \delta_r P_r - \int_{P_b}^{P_a} \delta dp, \quad (3)$$

where the subscripts a and r signify the surface of interest and a reference surface, respectively. Since this streamfunction is strictly applicable only for surfaces of constant  $\delta$ , ZHANG and HOGG (1992) have revised this formulation to reduce the errors on a surface of constant potential density. Their reformulation, which they term the "pressure anomaly streamfunction", is:

$$\psi_{M,a} - \psi_{M,r} = \delta_a P'_a - \delta_r P'_r - \int_{P_r}^{P_a} \delta dp, \quad (4)$$

where  $P' = P - \bar{P}$  and  $\bar{P}$  is the lateral mean pressure on the isopycnal surface. For our calculations we have adopted this latter form of the streamfunction. In computing the mean streamfunction at each gridpoint the specific volume anomaly and the pressure anomaly are computed from the mean P-T-S values. Dynamic heights are calculated for each station profile and then averaged at each gridpoint to produce the mean dynamic height that is used in Eq.(4).

For the prescribed reference level an assumed level of no motion has traditionally been used in studies of hydrographic data. The level of no motion is usually defined locally based on the local shear field and the measured or inferred flow direction. An assumption of a common level of motion for the entire North Atlantic basin is clearly inappropriate. Here we have selected the  $\sigma_2 = 36.90$  surface (with a nominal pressure of 2000db) as a reference level, so that our streamfunction represents the shear with respect to this surface. We restrict our computation of the streamfunction to the mid and upper thermocline surfaces ( $\sigma_0 = 26.50$  and  $\sigma_0 = 27.00$ ) where the geostrophic shear is large relative to the unknown reference level velocities.

In summary, the maps of potential temperature, salinity and oxygen, and pressure will be presented for all eight surfaces with the streamfunction maps presented for the upper two surfaces only. In an effort towards brevity, standard deviation maps are presented in each section for only pressure and temperature. Surfaces will be described sequentially from the uppermost to the deepest. This discussion focuses on basin scale characteristics and is intended to describe the general property patterns and circulation on each surface. Rather than restrict the discussion of the fields to the new features elucidated by this database, a brief overview of each field is given.

### 5.1 $\sigma_0 = 26.50$

#### *Water Properties: Fig.7*

This isopycnal surface outcrops in the winter along a line from Newfoundland to the northwest corner of Africa, and in the summer reaches nearly to Greenland and Iceland. Thus, the property fields exhibit large ranges in water mass characteristics. The intense temperature and salinity gradients, that extend eastward from Cape Hatteras and curve northward around the Tail of the Grand Banks, delineate a front between cold, fresh and warm, salty water masses. West and south of the Grand Banks these gradients mark the boundary between the Slope Water and Gulf Stream; to the north and east, the gradient is preserved by the contrast between the Mixed Water (WORTHINGTON, 1976; a water mass supplied by the southward flow of the Labrador Current) and the waters carried by the North Atlantic Current (NAC). The intensity of these gradients is maintained in the face of mixing by the strong advection of the Gulf Stream and the North Atlantic Current.

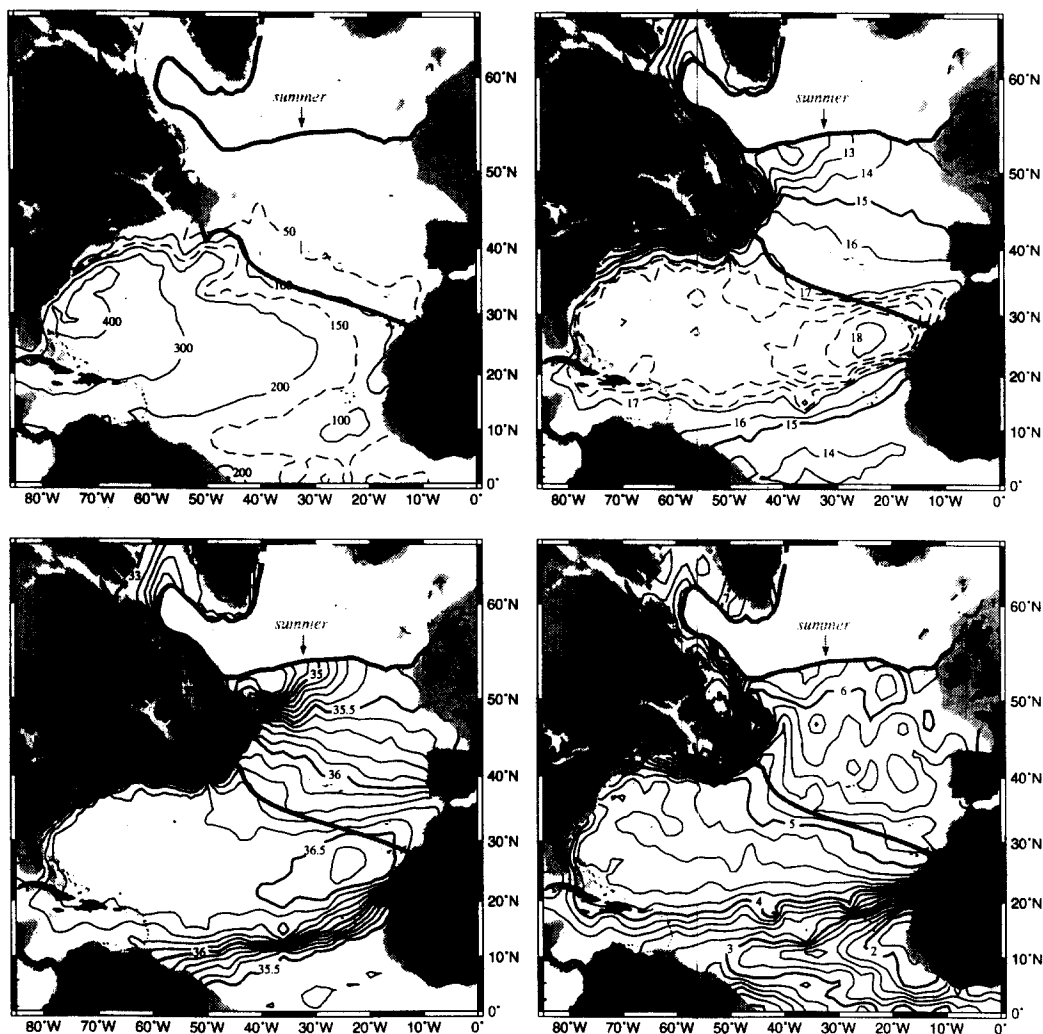


Fig.7. Mean properties for the  $\sigma_0=26.50$  surface. Bathymetry  $<200\text{m}$  is shaded gray on all 26.50 maps. Winter (Jan-Feb-Mar) and summer (Jun-Jul-Aug) outcrops of this surface are shown. For these and all subsequent maps the pressure units are db, temperature units are  $^{\circ}\text{C}$ , salinity is unitless and oxygen units are  $\text{ml l}^{-1}$ .

In contrast to those sharp gradients, a large pool of comparatively homogeneous water occupies the interior of the subtropical gyre. This Eighteen Degree Water (WORTHINGTON, 1959, 1976), a remnant of a deep winter mixed layer, is a variety of the global family of Subtropical Mode Waters (MCCARTNEY, 1982). West of  $50^{\circ}\text{W}$  the temperature and salinity of this water mass are exceedingly uniform ( $17.4^{\circ}\text{-}17.6^{\circ}\text{C}$  and  $36.4\text{-}36.5$ ) and match WORTHINGTON's (1959) definition of Eighteen Degree Water. East of  $50^{\circ}\text{W}$ , the Gulf Stream cools rapidly from  $17.4^{\circ}$  to  $17.0^{\circ}\text{C}$ , causing an eastward increase in the density of the Eighteen Degree Water (TALLEY and RAYMER, 1982). This change in density causes this mode water to lie above the 26.50 surface in the west and below it in the east, thus accounting for the eastward shoaling of this surface.

The subtropical gyre is bounded in the south by a front ( $15^{\circ}$  to  $20^{\circ}$ N), associated with the westward-flowing North Equatorial Current, which brings North Atlantic Central Water into contact with colder and fresher South Atlantic water. This extraequatorial position of the transition between South Atlantic and North Atlantic water masses occurs across the entire thermocline, as earlier observed by WORTHINGTON (1976).

The warmest and saltiest water on this surface lies in the closed contours near  $25^{\circ}$ N and  $25^{\circ}$ W. This water, Madeira Mode Water (SIEDLER, KUHLE and ZENK, 1987), derives its characteristics from a regional excess of evaporation over precipitation, coupled with Ekman layer convergence. In common with other mode waters, winter convection in this eastern region produces a substantial volume of subsurface water with a narrow range of characteristics. As with the deeper convective regime in the western Atlantic, this eastern region is bounded to the north by steep gradients of temperature and salinity, where the isopycnal is in the surface mixed layer, with the properties strongly influenced by surface fluxes of heat and fresh water. Figure 7 shows that the average winter outcrop lies to the north and northeast of this mode water. The warm, salty tongue of this mode water extends southwestward to approximately  $40^{\circ}$ W and also (potentially) influences the 27.00 surface, as will be seen in the next subsection. We note here that the streamlines (discussed below) in the vicinity of this water mass significantly cross mean isotherms, suggesting that there must be significant diffusion to balance mean advection.

The sea surface influence is particularly apparent in the oxygen field for  $\sigma_0 = 26.50$ . High values of oxygen ( $6\text{-}8\text{ml l}^{-1}$ ) are found in the shallow regions of this isopycnal, with the Slope Waters and the Mixed Waters in the Labrador Sea having the highest oxygen values. Other than the sharp gradient produced by the contrast of these highly oxygenated waters with the interior waters, the pattern of the oxygen field is quite different from that of the salinity and temperature fields. The subtropical gyre is not homogenized, there is no evidence of Madeira Mode Water and the oxygen field in the northeast region lacks the broad, uniform gradient seen in the temperature and salinity fields. The most striking feature of this oxygen field is the presence of a low oxygen tongue that extends from the west coast of North Africa westward to South America along an axis at  $\sim 12^{\circ}$ N. The extremely low oxygen values in this vicinity are attributed to a combination of biological and physical effects. Strong upwelling off the west coast of North Africa (TOMCZAK, 1980) generates intense consumption of oxygen beneath the euphotic zone. Because these waters are neither locally ventilated, or replenished by freshly-subducted waters, there is no strong source of oxygen to balance the consumption resulting from upwelling at these depths.

An interesting feature in the region south of the Gulf Stream is the clockwise torquing of the oxygen contours. In the west a low oxygen tongue sweeps east-northeast from Cape Hatteras along the southern flank of the Gulf Stream. This contrasts with relatively higher oxygen values (a result of surface contact) that are swept southwestward with the recirculation (TALLEY and RAYMER, 1982; MCCARTNEY, 1982) from the region south of the Grand Banks (where this surface has moved above the Eighteen Degree Water). The relatively low oxygen values result from the combined influence of the eastern tropical oxygen minimum waters (noted above) and the low-oxygen North Brazil Current which supplies water to the North Atlantic through the Caribbean to partially feed the Florida Current (SCHMITZ and RICHARDSON, 1991).

#### *Circulation: Figs 7 and 8*

The circulation on this surface is dominated by the large scale subtropical gyre as seen in the pressure field, reaching to a maximum of 400db in the western domain. The gyre is bounded to the west and north by the swiftly-moving Florida Current and Gulf Stream, respectively, to the east by a weak southward flow, and to the south by a broad westward return flow. This return flow

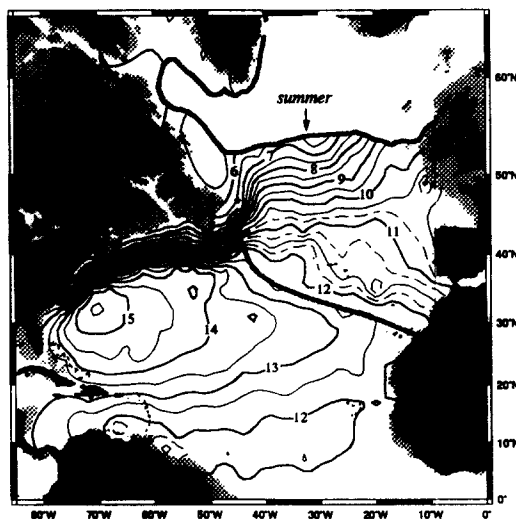


Fig.8. Mean streamfunction for the  $\sigma_0=26.50$  surface. For this and all subsequent streamfunction maps the units are  $\text{m}^2\text{s}^{-2}$ . The contour interval is  $0.5\text{m}^2\text{s}^{-2}$ , except in the eastern basin where the 10.75, 11.25 and 11.75 contours have been added for clarity.

supplies the Florida Current, as it flows northward from near the Florida Straits and then along the east coast of North America. Tightly compressed streamlines clearly identify the Florida Current's seaward extension, the Gulf Stream. The Stream's mean width, estimated by the distance between the 100 and 400db contours near  $70^\circ\text{W}$ , is approximately 300km, exceeding the width of the instantaneous Gulf Stream by a factor of two. We attribute this broadening to the temporal meandering of the synoptic Gulf Stream and not the spatial smoothing of our database: both FUGLISTER's (1963) survey and an analysis of satellite images (CORNILLO, 1986) show that the Gulf Stream meanders over a 500km envelope, which is considerably larger than the 100km scale over which we smoothed our data.

The streamfunction field delineates a bifurcation of the Gulf Stream near  $45^\circ\text{W}$ , with a portion of the Gulf Stream, loosely defined by streamfunction contours 11-13, extending southeastward into an Azores Current. The progressive peeling off of the contours to the south represents the recirculation of the Eighteen Degree Water that is carried eastward by the Gulf Stream and constitutes the slow, broad interior flow of the subtropical gyre. This southward flow, which extends to nearly  $20^\circ\text{W}$ , turns westward near  $20^\circ\text{N}$  to complete the gyre. The streamfunction map shows that the Azores Current survives the divergence of the subtropically recirculated waters and is seen to extend eastward well beyond  $20^\circ\text{W}$ . Interestingly, near  $15^\circ\text{W}$  there is a convergence of flow into the Azores Current from the northwest (represented by the 10.75-11.25 streamfunction contours), which creates a broad southeastward flow over an area defined by  $30^\circ$  to  $40^\circ\text{N}$  and  $5^\circ$  to  $20^\circ\text{W}$ . The picture of the Azores Current which emerges from our maps is one of a coherent flow that occupies almost half the basin's width. Waters diverge to the south as the Azores Current branches from the Gulf Stream, but this divergence is partially matched further east by converging flow from the north. The reader is referred to STRAMMA and SIEDLER (1988) for a quantitative discussion of the upper circulation in this eastern region and to MANN (1967), KLEIN and SIEDLER (1989) and KRAUSS, KASE and HINRICHSSEN (1990) for details concerning the branching of the Gulf Stream and the origin of the Azores Current.

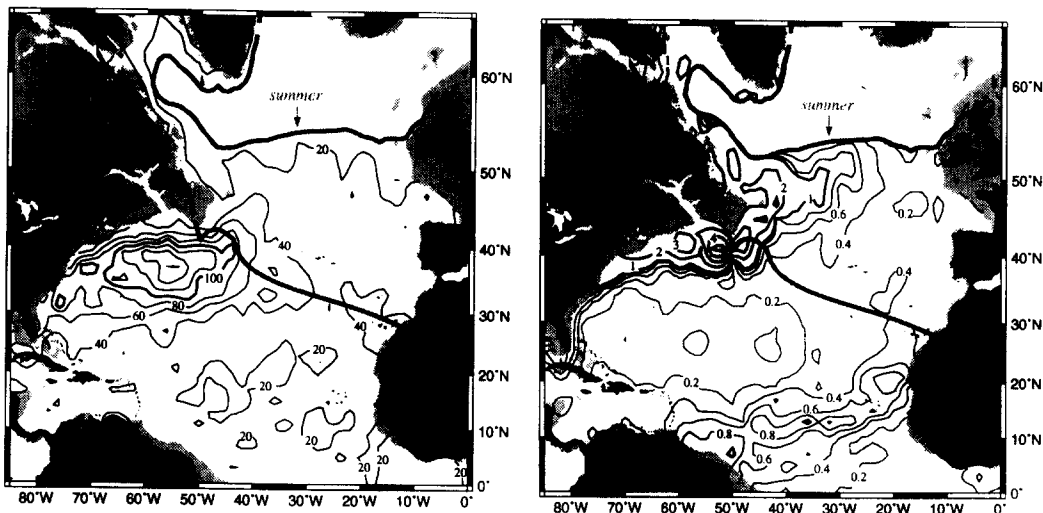
*Variability: Fig.9*

Fig.9. Standard deviations for the  $\sigma_0=26.50$  surface. For these and all subsequent standard deviation maps the pressure units are db and temperature units are  $^{\circ}\text{C}$ .

The largest temperature variability occurs in those regions where the temperature contrast is the greatest; namely, in the vicinity of the Gulf Stream, the North Atlantic Current and in the Labrador Sea. In areas with strong horizontal gradients, small lateral migrations of the isopycnal surface can produce large property variations at a fixed geographic locale. Thus, the strong variability in the Gulf Stream and the NAC is primarily attributed to the strong temporal meandering of these currents. The variability in the Labrador Sea, however, results mainly from the shallow depth of this surface and the strong seasonal variability in this region. Finally, low variability in the interior reflects the vertical and horizontal homogeneity of the mode waters present there.

The variability of the pressure field is dominated by high values in the vicinity of the Gulf Stream. Given the 300m shoaling across the Gulf Stream, standard deviations on the order of 100m are consistent with the meandering of the entire stream past a fixed point. The increased variability east of the New England Seamounts is possibly related to a broadening of the current past the seamounts and/or to the interannual variability of the Eighteen Degree Water (TALLEY and RAYMER, 1982). We favor the latter explanation because the maximum variability of the pressure field occurs on the southern flank of the Gulf Stream near the formation region of this water mass. Because of its very weak vertical density gradient, small changes in the Eighteen Degree Water can cause the isopycnal to shift vertically 300m. Finally, in the northern portion of the basin, seasonal outcropping of this surface causes the standard deviation values to approach the values of the mean pressures.

5.2  $\sigma_0 = 27.00$ 

## Water Properties: Fig.10

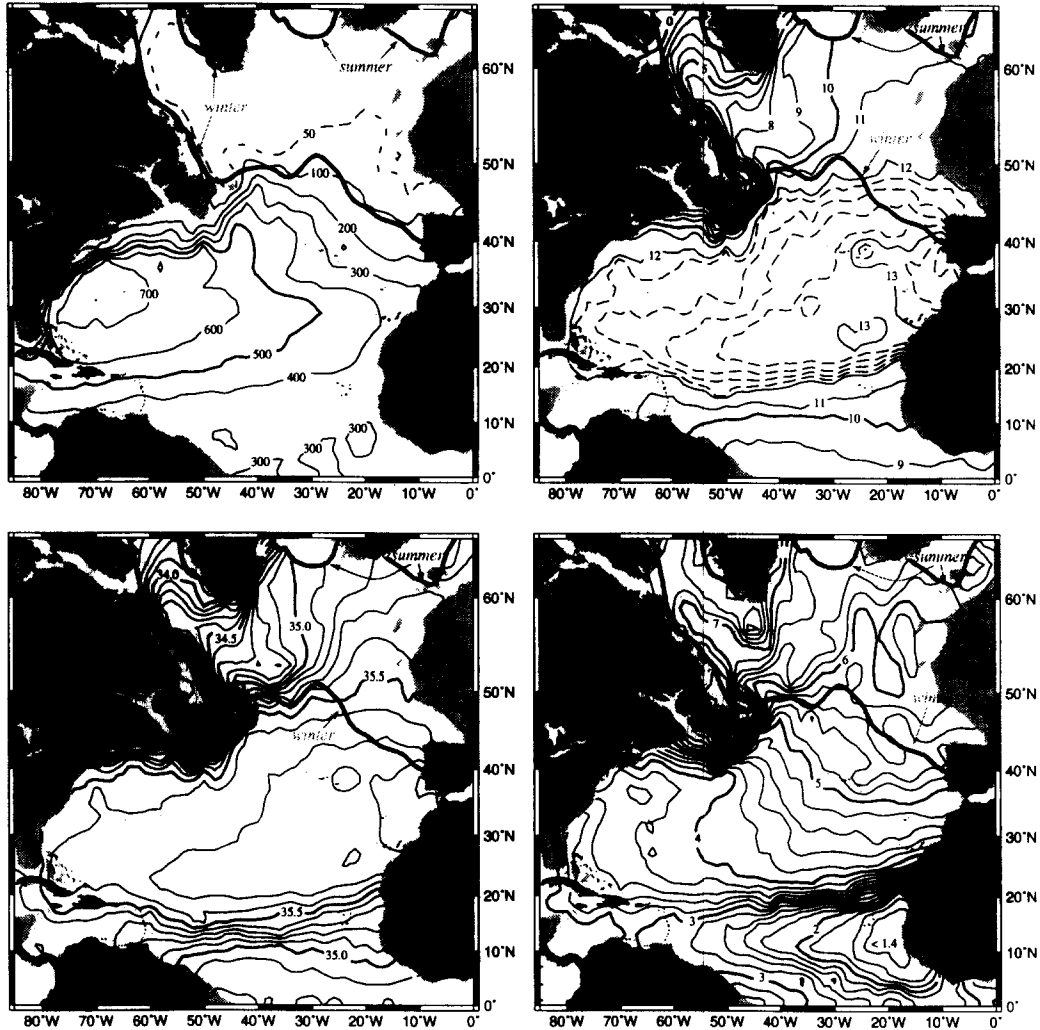


Fig.10. Mean properties for the  $\sigma_0=27.00$  surface. Bathymetry  $<200\text{m}$  is shaded gray on all 27.00 maps. Winter (Jan-Feb-Mar) and summer (Jun-Jul-Aug) outcrops of this surface are shown. The peculiar shape of the oxygen 6.0 contour in the area between the winter and summer outcrops likely reflects a sampling bias, rather than a true climatological feature.

On this surface the waters of the subtropical gyre are also bounded to the north by sharp gradients separating coastal waters from the Gulf Stream/NAC system and to the south by the transition between North Atlantic and South Atlantic waters. Two differences between this surface and the one previously discussed are noted: With a nominal temperature of  $12.5^\circ\text{C}$  in the gyre interior, this surface is beneath the Eighteen Degree Water that dominates the 26.50 surface, and thus lacks a broad scale uniformity of the temperature and salinity fields in the western subtropical

gyre. Another difference on this surface is the presence of a geographically-limited, warm and salty tongue emanating from the Straits of Gibraltar. Because at this pressure (200-300db) there is a net inflow into the Mediterranean, this tongue is not the result of the overflow waters that will be seen to dominate the deeper surfaces. Instead, it is postulated that these characteristics are a signal of locally-subducted waters, as suggested by the location of the winter outcrop to the north of this feature. Alternatively, it is suggested that the waters on this surface mix with the underlying Mediterranean outflow, becoming progressively warmer and more saline as they flow toward the Straits of Gibraltar.

A closed contour region (13°C and 35.7) in the eastern domain centered on 22°W and 27°N is notable on this surface, not because of its extent or strength, but rather its location. This patch of warm and salty water lies just beneath the Madeira Mode Water noted for the 26.50 surface. Since the nominal pressure at this locale is approximately 400db and since the winter outcrop for this surface is located near 24°N, it is postulated that this local homogeneity is a result of vertical mixing processes rather than direct convection to this depth. Supporting this supposition is the lack of sharp gradients to the north of the warm patch that would indicate the approach of the surface to the outcrop. Alternatively, this patch could be a climatological manifestation of the anomalously warm and salty lenses of Mediterranean Water (Meddies) that populate this region (ARMI and ZENK, 1985). This patch is centered on the corridor for Meddies, which extends southwestward from Cape St Vincent, Portugal, as determined by RICHARDSON, MCCARTNEY and MAILLARD (1991) from a survey of historical hydrographic data. Since Meddies are commonly centered near pressures of 1000db and extend over 800db, this surface (with a mean pressure at this locale of approximately 450db) would sample only the upper reaches of the Meddies. Perhaps this surface would more likely sample shallow Meddies, whose anomalous signals have been found by PINGREE and LECANN (1993) to extend to the surface waters. We end the discussion of this feature by noting that a further examination is warranted to determine whether the closed 13°C contour region is associated with the 13°C water to its east. If such is the case, this feature could simply reflect an advective-diffusive tongue of the locally-subducted waters or of the Mediterranean inflow waters, as discussed above.

The penetration of the low oxygen waters from the tropics into the western North Atlantic, noted for the previous surface, is most prominent on this surface. The 3.0 and 3.1 ml l<sup>-1</sup> contours trace the path of these waters through the Caribbean and along the southeastern US coast. The tongue of low oxygen is particularly evident as these waters are advected seaward as part of the Gulf Stream and NAC. Also of note from the oxygen field are the highly oxygenated surface waters in the northern domain and the low oxygen waters off the northwest coast of Africa, associated with the upwelling previously discussed.

#### *Circulation: Figs 10 and 11*

Because this surface is less influenced by seasonal outcropping than the preceding one, its pressure field is more representative of the topography of the main thermocline over a substantial part of the subtropical gyre. Notably absent is the eastward shoaling of the isopycnal along the southern edge of the Gulf Stream that marked the Eighteen Degree Water on the 26.50 surface. On this surface the isopycnal rises uniformly 400m to the north from Cape Hatteras to approximately 45°W, thus defining the Gulf Stream. Although the width of the Gulf Stream is similar to that for the shallower surface, the relative velocities are approximately half, an indication of the strong shear in the thermocline.

Near 50°W there is a southward branching of the Gulf Stream. This flow trends southeastward until near 30°N where it turns southwestward toward Puerto Rico, thus closing the subtropical

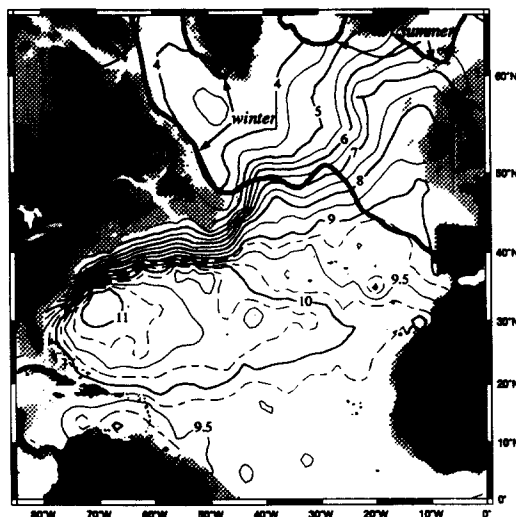


Fig.11. Mean streamfunction for the  $\sigma_0=27.00$  surface. The contour interval is  $0.5\text{m}^2\text{s}^{-2}$  north of  $40^\circ\text{N}$  and  $0.25\text{m}^2\text{s}^{-2}$  south of  $40^\circ\text{N}$ .

gyre. Compared to the lighter surface, the subtropical bowl for this surface shows a slight contraction to the north and west (WORTHINGTON, 1976; REID, 1978). Little southward subtropical flow is found east of  $30^\circ\text{W}$  on this surface. This observation is consistent with SAUNDERS' (1982) inference of an upper water column concentration of the Sverdrup transport in the eastern basin. Past  $50^\circ\text{W}$  the colder components of the Gulf Stream turn northward around the Tail of the Grand Banks and converge into the North Atlantic Current. Near  $40^\circ\text{N}$  the 9.5 and 9.75 contours define the Azores Current on this surface. After it branches from the main part of the Gulf Stream extension, this current flows southeastward south of the Azores islands, lying just beneath the expression of the Azores Current on the 26.50 surface.

After the Azores Current separates, the North Atlantic Current flows northeastward, seaward of the Flemish Cap ( $47^\circ\text{N}$ ,  $45^\circ\text{W}$ ), to near  $50^\circ\text{N}$ . Here, the North Atlantic Current (NAC) turns eastward and becomes a much more diffuse flow, commonly called either the North Atlantic Drift or Current (KRAUSS, 1986). The contours that define this flow broaden near the crest of the Mid-Atlantic Ridge. The sharpness of this divergence has not been particularly apparent in recent circulation diagrams (e.g. SY, 1988; SCHMITZ and MCCARTNEY, 1993), but is consistent with the transport scheme of DIETRICH, KALLE, KRAUSS and SIEDLER (1975). The warmer components continue eastward and then (eventually) turn southward, while the colder components turn to the northeast. This divergence implies that at this depth a significant fraction of the waters of subtropical origin are diverted southward. Thus, the supply waters for the northern Atlantic are primarily of subpolar origin, as can be seen in Fig. 11. The northward flow stems mainly from the waters carried by the Labrador Current that are recirculated into the NAC near  $45^\circ\text{N}$ . We note, however, that since the streamfunction contours on this surface mainly represent the seasonal mixed layer waters in the subpolar gyre, this partitioning is not definitive.

In a recent paper by SY, SCHAUER and MEINCKE (1992) a synoptic section across  $26^\circ\text{W}$  shows that several jets occupy the region from  $45^\circ$  to  $52^\circ\text{N}$ . The broad climatological flow of the NAC past the Mid-Atlantic Ridge is perhaps the manifestation of these jets collectively meandering in

this locale. However, there is at least one indication in our fields that these individual synoptic jets have climatological counterparts. We note that the 9.0 to 9.25 contours, centered near 46°N in the eastern basin, form a coherent eastward jet (until near 15°W) that may be the climatological manifestation of the synoptic jet noted by KRAUSS (1986) along 47°N. Interestingly, it is the southward flow of this branch that joins the eastward extension of the Azores Current near 15°W and matches the convergence of northern waters feeding into the Azores Current noted on the lighter surface.

*Variability: Fig.12*

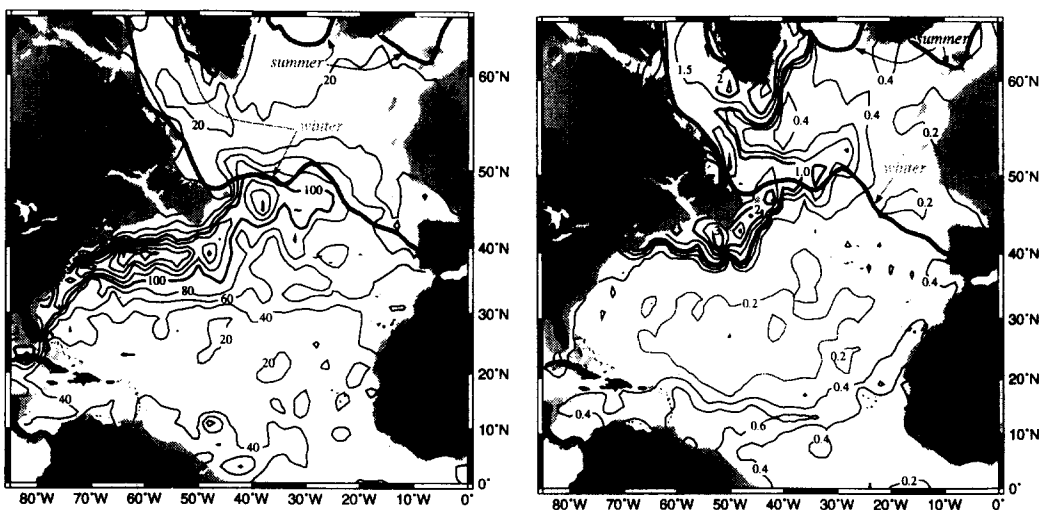


Fig.12. Standard deviation fields for the  $\sigma_0=27.00$  surface.

The standard deviation map for pressure shows the expected high variability along the paths of the Gulf Stream and the North Atlantic Current, with a maximum centered at 38°W and 46°N, the locale where the NAC essentially retroflects into an eastward flow. Saddles of low variability are evident at 50°W and just south of the Flemish Cap, possibly reflecting the relative stability of the frontal position of the Gulf Stream/NAC just before and after the bifurcation of the flow at the Tail of the Grand Banks. A weak minima is also noted near 68°W, which is the site of a permanent trough in the Gulf Stream, as measured from satellite images (LEE, 1994). Also of note on this surface is the tongue of high temperature variability that extends eastward from the Labrador basin. Because the Labrador current system is a source of strong thermohaline anomalies (AHRAN, 1990), this tongue reflects the eastward spreading of Labrador Current water into the North Atlantic Current.

5.3  $\sigma_t = 31.85$ 

Water properties: Fig. 13

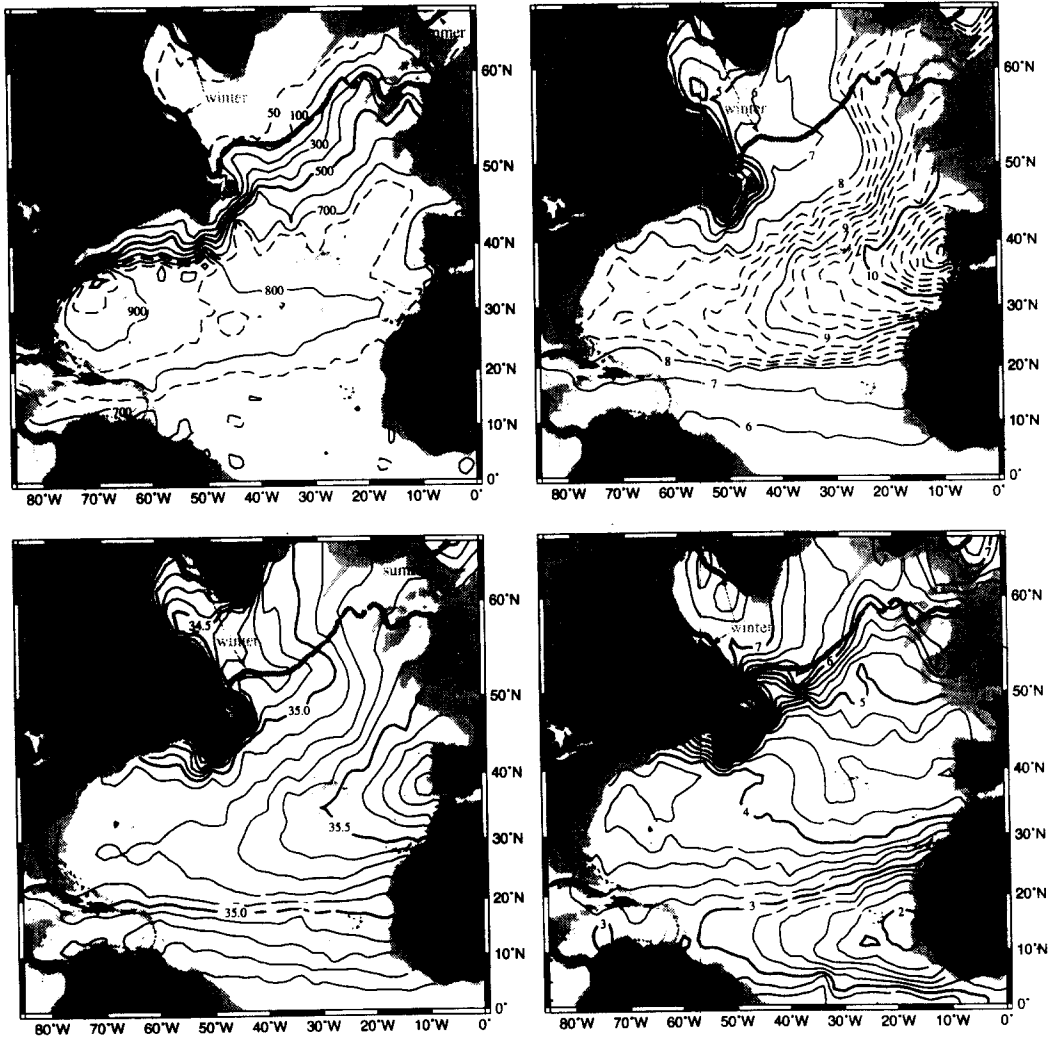


Fig. 13. Mean properties for the  $\sigma_t=31.85$  surface. Bathymetry  $<1000\text{m}$  is shaded gray on all 31.85 maps. Winter (Jan-Feb-Mar) and summer (Jun-Jul-Aug) outcrops of this surface are shown.

Except for the regions north of  $50^\circ\text{N}$ , this isopycnal lies well below the surface mixed layer, with a maximum pressure of  $\sim 950\text{db}$  in the subtropical gyre. The temperature and salinity fields in the subtropics are clearly dominated by the intrusion of warm, salty water from the Mediterranean outflow into the basin interior. The characteristic warm and salty signal spreads westward from the eastern boundary across the entire basin, spanning nearly  $20^\circ$  of latitude. This water mass contrasts sharply with the cooler and fresher waters carried by the Gulf Stream/NAC and with the colder and fresher waters of the South Atlantic. The temperature and salinity gradients in the subtropical gyre reflect the advective-diffusive balance between these waters, producing a Mediterranean signal

that weakens to the west. This contrasts sharply with the temperature and salinity fields for the 26.50 surface where the dominance of a single water mass (Subtropical Mode Water) is responsible for the uniformity of the fields.

Although the Mediterranean tongue geographically dominates this surface, the strongest water mass contrast is in the Labrador Sea. The cold, fresh waters carried southward by the Labrador Current about the warmer and saltier waters carried northward by the North Atlantic Current, creating the sharp gradient situated off the eastern coast of Canada. This gradient is less pronounced for this surface than for the previous surfaces because the NAC waters are considerably cooler relative to the surfaces above, while the onshore waters are of comparable temperature. Because no Slope Water is present on this density surface, the temperature and salinity contrast across the Gulf Stream is considerably reduced. The Mixed Water (WORTHINGTON, 1976) west of the North Atlantic Current off the Grand Banks of Newfoundland maintains the temperature contrast in that region.

The oxygen field for this surface is marked by high values in the entire northern domain, reflecting the contact with the atmosphere of the cold mixed layers in this portion of our domain. Since this surface deepens several hundred meters to the east, the pronounced east/west oxygen gradient can be attributed to the increasing isolation of this surface from the sea surface. Because oxygen is more soluble in colder waters, the oxygen gradient perhaps also reflects the large east-west temperature gradient in the subpolar gyre on this surface; the temperature rises from nearly 0°C to 9°C, running west to east. On this surface it is evident that the lower oxygens from the subtropical region and the higher oxygens from the subpolar region lie on the offshore and onshore sides, respectively, of the North Atlantic Current. When the NAC turns northward, near 25°W, the oxygen isopleths are no longer aligned with the flow, rather the oxygen contours (5.0 - 6.2 ml l<sup>-1</sup>) lie perpendicular to the streamlines in the northeast corner. This configuration suggests that there is *in situ* convection in this vicinity, in agreement with MCCARTNEY and TALLEY's (1982) assessment that a variety of Subpolar Mode Water is formed in this locale. On our maps the increase in oxygen following the flow reflects the progressive penetration of convection reaching this surface.

A related signature is seen in the temperature and salinity fields. As the North Atlantic Current flows toward the mode water formation region off Ireland, the temperature and salinity rise perceptibly. This has been taken as an indication (REID, 1978) of the influence of the Mediterranean Water on the warm water entering the subpolar gyre, and ultimately on the Norwegian Current, via an eastern boundary current. An alternate explanation is that the progressive cooling (driven in large part by an evaporative heat flux) of the Subpolar Mode Water is mixing downwards (in density) the higher salinities of the lighter density surfaces, producing the order 0.2 salinity difference along streamlines connecting the Newfoundland area to the Ireland area. Considering the proximity of the Mediterranean outflow waters to the northward-flowing NAC, we also raise the third possibility that diffusive fluxes influence the property change along the path of the NAC.

The tongue of low oxygen water spreading westward from the upwelling region off northwest Africa is also evident on this surface, albeit weaker. The oxygen values near the African coast are approximately 0.2 ml l<sup>-1</sup> higher than the surface above, indicating that either at this pressure (800db) the biological uptake of oxygen is not as great or there is a difference in the replenishment of oxygen via advection and/or mixing. For the subtropical gyre the waters on this surface are generally poorer in oxygen than the waters on the surface above. In fact, because the waters near the outcrop region for this surface do not subtropically recirculate (MCCARTNEY, 1982), this surface is near the oxygen minimum within the subtropical gyre. Finally, the clockwise torquing of the oxygen field in the western subtropical basin, discussed for the shallower surfaces, is evident here as well.

---

*Circulation: Fig.13*

For the interpretation of flow on this surface, and for all subsequent surfaces, the pressure map will be used in conjunction with assumed levels-of-no-motion to give a qualitative description of the overall flow pattern. Future plans include an assessment of these flow fields based on more objective means. For this surface, and the next four surfaces, a deep level-of-no-motion is assumed for the subtropical circulation, including the Gulf Stream and its extension into the NAC. A reference level shallower than this surface is assumed for the Deep Western Boundary Current (DWBC) (HOGG, PICKART, HENDRY and SMETHIE, 1986; MCCARTNEY, 1993; MOLINARI, FINE and JOHNS, 1992) for the tropics and for the eastern basin. For the interpretation of the subpolar region, a mid-depth level of minimum speed is used in accordance with the work of IVERS (1975) and MCCARTNEY (1992), such that for much of the subpolar gyre the flow is cyclonic throughout the water column.

On this surface the continuity between the Gulf Stream and the NAC is apparent in the pressure field. Near 50°W a branch of the Gulf Stream turns southward and is recirculated as part of the subtropical gyre. At this depth the southward return flow is weak, as measured by the rise of the isopycnals to the east and south. The Gulf Stream flows eastward past the divergence of the subtropically-recirculated waters, until near 45°W where it turns around the Tail of the Grand Banks and continues as the NAC. Neither an Azores Current nor a 47°N jet is discernible on this surface. As seen in the pressure field, at the bifurcation near 50°W the southward branch is small relative to the continuation, thus it *appears* that more subtropical waters are sent northward than recirculate. This reflects the dominance of transport near this surface in the supply of warm water from the subtropical gyre to the subpolar gyre, where it is the source water for the production of denser waters by cooling in the Nordic Seas (WORTHINGTON, 1970) and the subpolar gyre (MCCARTNEY and TALLEY, 1984). Although it is not marked by the same divergences as in the surfaces above, the NAC on this surface, as with the upper surfaces, shows a strong convergence near 45°N, where the southward-flowing Labrador Current partially feeds into the northward-flowing NAC. Finally, our reference level choice for the eastern basin leads to an interpretation of cyclonic flow around the Mediterranean tongue from 30°N to 45°N. However, because this reference level choice for the eastern basin is at best tentative, further studies are warranted before the climatological flow in the vicinity of the Mediterranean outflow can be estimated.

*Variability: Fig.14*

The variability of temperature and salinity on this surface is largest along the coastal boundary from near Nova Scotia north to the Labrador Sea, where the property gradients are maximized on this surface. Particularly large variabilities are located at the Tail of the Grand Banks, a region of intense mixing (SCHMITT and GEORGI, 1982). Elsewhere on this surface there is markedly low variability, with values on the order of 0.2°C for temperature. Values <0.2°C are found in the northeast subpolar gyre, reflecting the occupation of Subpolar Mode Water in this locale. Slight elevations are noted in the vicinity of the Mediterranean outflow, off the northwest coast of Africa (near the region of intense surface upwelling) and east of the windward islands.

Pressure variabilities are large in the vicinity of the Gulf Stream and the North Atlantic Current, with the variance pattern generally following the path of these two currents. Coincident with the *low* property variability in the northeast corner of the domain is a *high* pressure variability (on the order of 140db). In this region, which is characterized by low vertical density gradients, seasonal and interannual variability of the Subpolar Mode Water can cause large vertical excursions of the isopycnal. Thus, the standard deviations in the northern extent of the domain are comparable in

strength to the mean pressures. This contrasts with the interior where, for nominal pressures of 800 to 900db, the standard deviations are only 40db. Additionally, this recalls the Subtropical Mode Water discussed earlier, where high *pressure* variabilities are associated with low *property* variabilities, as found along the southern flank of the Gulf Stream on the 26.50 surface.

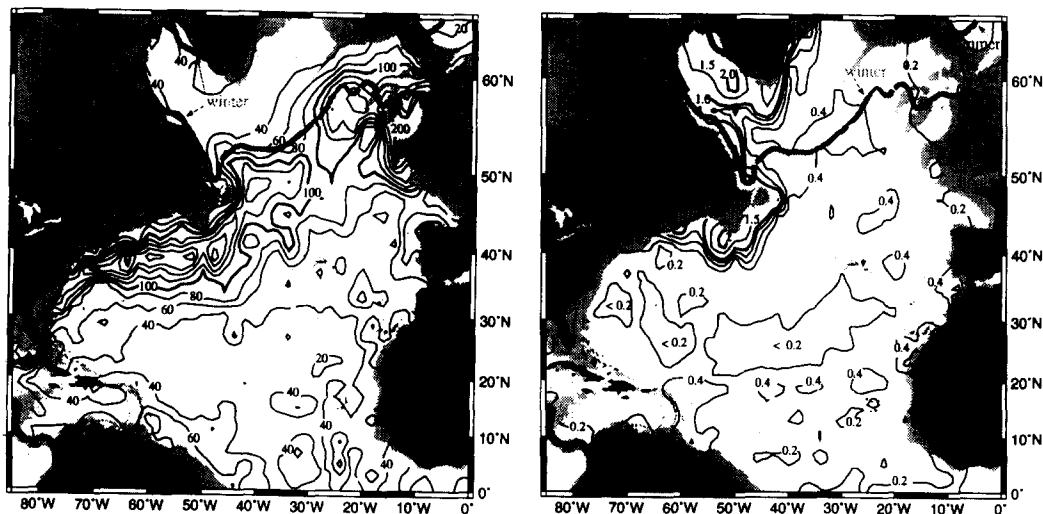


Fig.14. Standard deviation fields for the  $\sigma_t=31.85$  surface.

#### 5.4 $\sigma_t = 32.35$

##### *Water properties: Fig.15*

Unlike shallower surfaces, this isopycnal surface does not have a sharp thermal or haline front associated with either the Gulf Stream, the North Atlantic Current, or the Equatorial Countercurrent. Instead, the warm tongue of Mediterranean Water extending from the eastern Atlantic basin completely dominates the property fields of the subtropics. The strength of the tongue is maximized at this depth, changing by 4°C and by almost 1 unit in salinity from the east coast to the west coast. Also of note are the two cold and fresh water masses bracketing the Mediterranean tongue. Labrador Sea Water (3.4°-3.6°C and 34.86-34.88) fills the northwest corner of the domain while South Atlantic waters (4.2°C and 34.98) extend to approximately 15°N.

This surface marks another transition in that the oxygen field has a pattern similar to the temperature field, indicating the decreasing influence of surface processes and the increasing influence of advection and mixing of waters from only a few sources. Compared to the upper three surfaces the range of oxygens on this surface is considerably reduced; the highest values (6.6-6.7ml l<sup>-1</sup>) occur in the Labrador Sea and the lowest values (4.4-4.8ml l<sup>-1</sup>) occur in the (previously discussed) upwelling region off the African coast. This area of low oxygens is shifted northward from the above surfaces (LEVITUS, 1982). The 5.6ml l<sup>-1</sup> contour in the western basin marks the southward penetration of the high oxygen Labrador Sea Water, consistent with the work by TALLEY and MCCARTNEY (1982). Additionally, an intrusion of high oxygen values (5.2-5.4ml l<sup>-1</sup>) from the South Atlantic is evident in the tropical region, particularly in the western basin.

Circulation: Fig.15

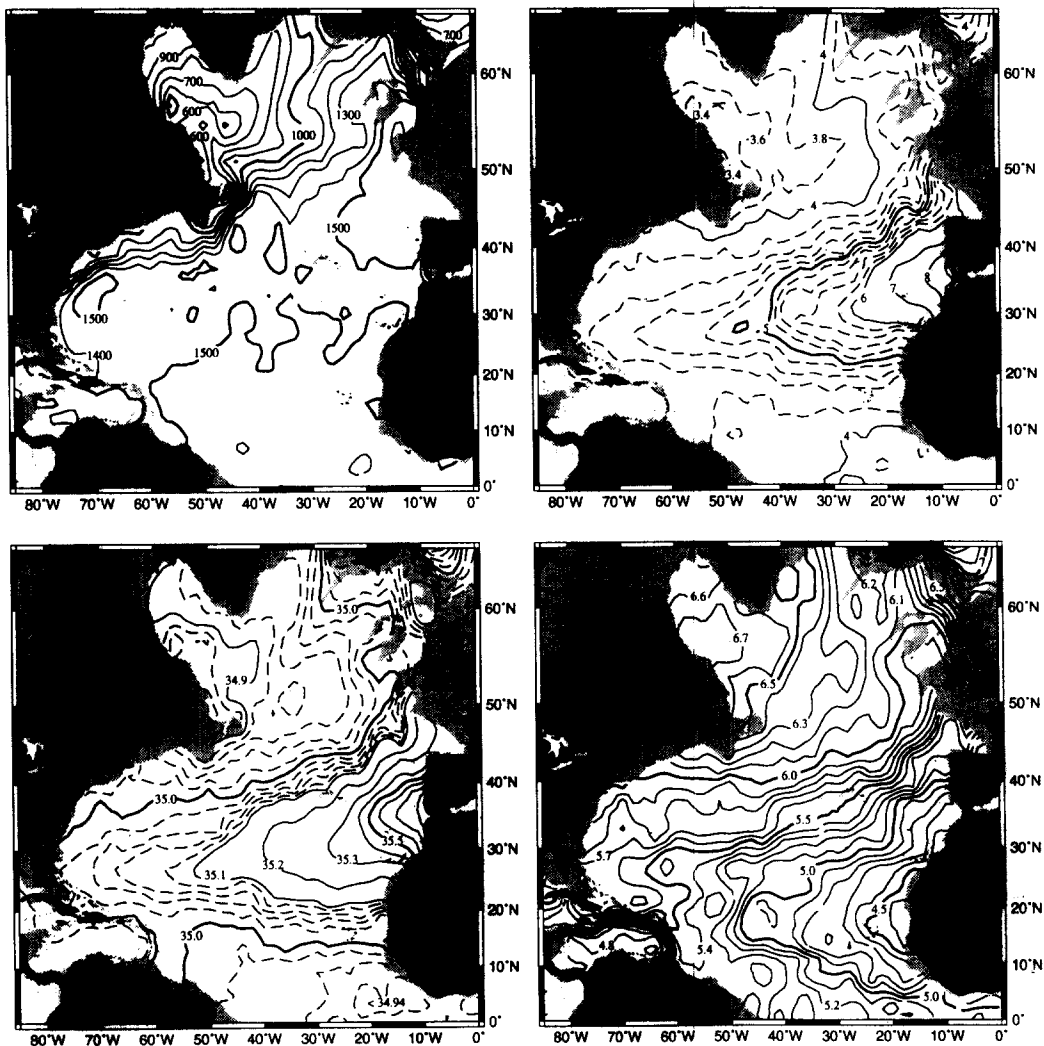


Fig.15. Mean properties for the  $\sigma_t=32.35$  surface. Bathymetry  $<1000\text{m}$  is shaded gray on all 32.35 maps.

For the interpretation of flow on this surface we assume the same reference levels as for the preceding surface: a deep level-of-no-motion is assumed for the subtropical circulation, including the Gulf Stream and its extension into the NAC. A reference level shallower than this surface is assumed for the DWBC, the tropics and the eastern basin and a mid-depth level of minimum speed is used for the subpolar region. The Gulf Stream, and its continuation into the NAC, is evident on this surface, although the ambiguity of a reference level prevents a clear assessment of where the shear signals signify the eastward/northward-flowing Gulf Stream/NAC decreasing with depth or the southward/westward flowing DWBC increasing with depth. The lack of vertical shear on this surface south of the Gulf Stream is consistent with SCHMITZ's (1980) characterization of this

region as the weakly-depth dependent segment of the North Atlantic, where the inertial recirculation is primarily barotropic. On the other hand, in the eastern basin the lack of vertical shear has been interpreted by SAUNDERS (1982) to signify weak absolute flow at this depth.

The southern extent of the subpolar gyre on this surface is more clearly delineated in the northwestern portion of the domain with the 700-1000db contours marking the southward penetration of the subpolar gyre along the western continental boundary. As with the 31.85 surface the isobars indicate that this southward-flowing Labrador Sea Water retroflects northward near the Flemish Cap and joins the NAC; a pattern that was noted by CLARKE, HILL, REININGER and WARREN (1980) in their analysis of synoptic hydrographic data. The convergence of these two currents causes the colder components of the NAC to become slightly cooler, through mixing: south of the Grand Banks the 1000 to 1400db contours are associated with the 3.8° to 4.2°C contours: Where the NAC retroflects these same isobars are associated with 3.6° to 4.0°C waters. Furthermore, the eastward displacement of the 3.8°C contour forms a cold tongue that matches TALLEY and MCCARTNEY's (1982) inference that Labrador Sea Water flows eastward with the NAC. This suggests that the relatively high oxygen values in the northeast domain are derived from the advection of highly-oxygenated water from the Labrador Sea. This penetration of the Labrador Sea Water to the eastern boundary near 52°N (Porcupine Bank) has been demonstrated in a synoptic section by AHRAN, COLIN DE VERDIERE and MEMERY (1994).

*Variability: Fig.16*

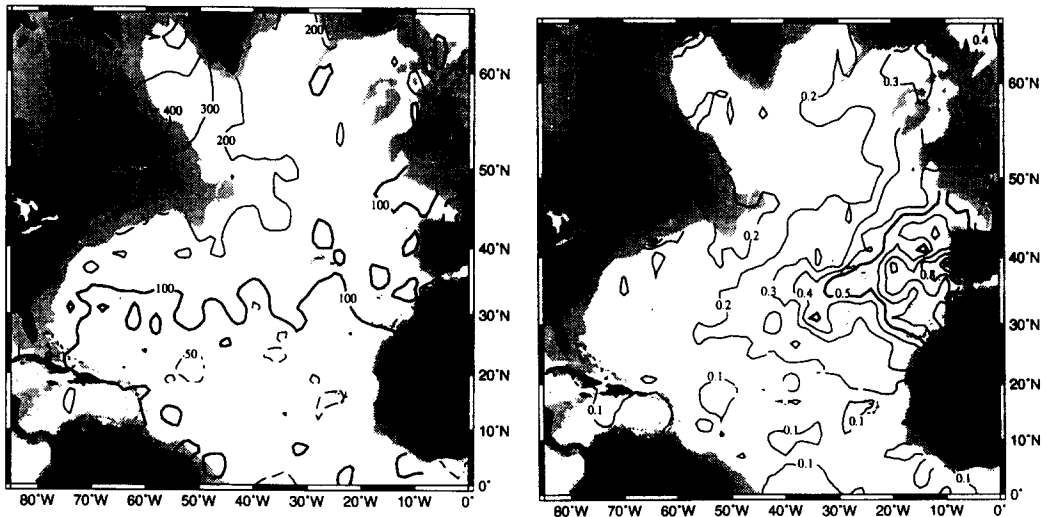


Fig.16. Standard deviation fields for the  $\sigma_1=32.35$  surface.

The map of temperature variability is relatively flat, with the largest deviations ( $\sim 0.6-0.8^\circ\text{C}$ ) occurring in the vicinity of the Mediterranean tongue. Elsewhere the variability is  $< 0.2^\circ\text{C}$ , reflecting the uniformity of the waters at this depth. This surface lacks a strong pressure variability in the northeastern domain (found on the previous surface), suggesting it is below the convective range for the formation of the mode waters in that region. Instead, the pressure variability on this surface is dominated by large values (300db) in the Labrador Sea, consistent with TALLEY and MCCARTNEY's (1982) finding that this surface contains the classical Labrador Sea Water.

5.5  $\sigma_2 = 36.95$

Water properties: Fig.17

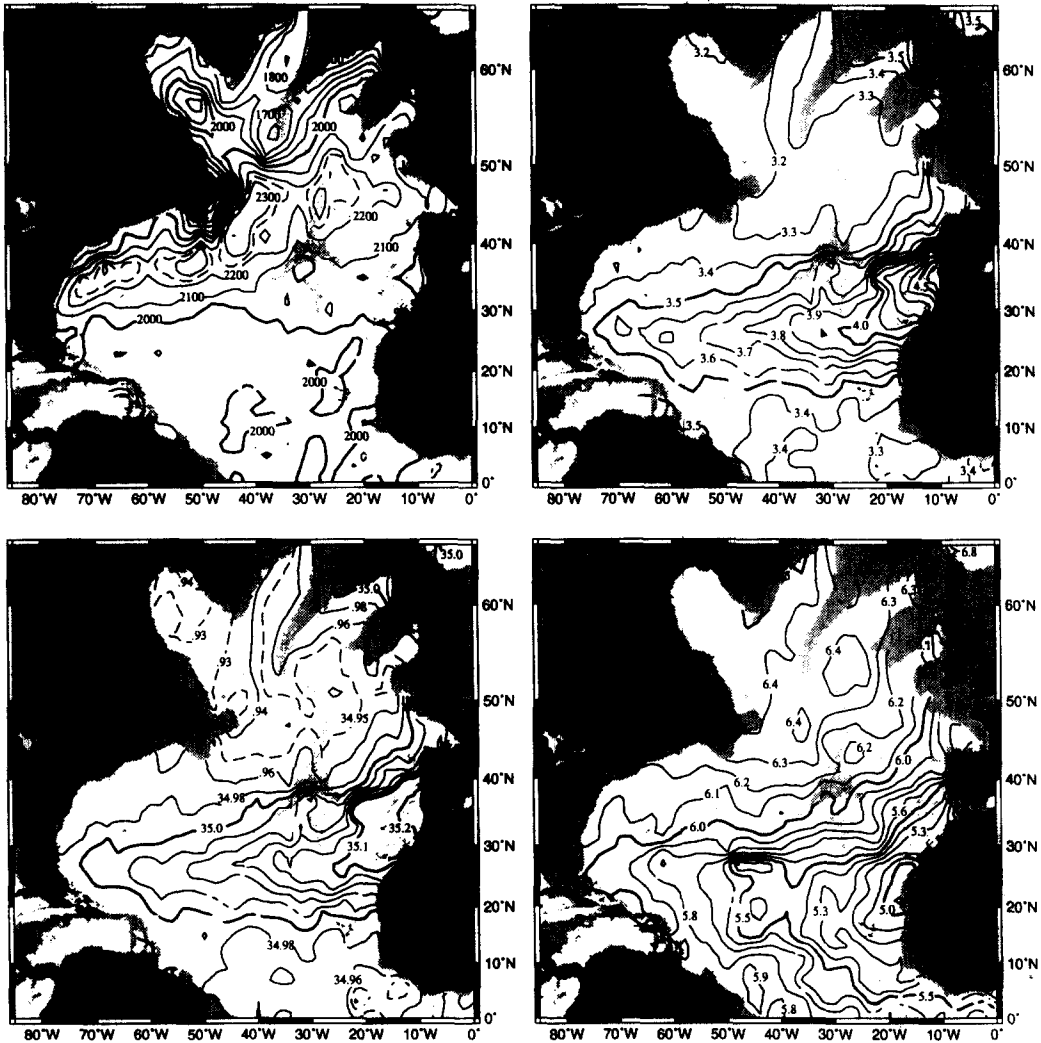


Fig.17. Mean properties for the  $\sigma_2=36.95$  surface. Bathymetry  $<2000\text{m}$  is shaded gray on all 36.95 maps.

Three water masses can be identified on this surface: North Atlantic Deep Water occupies the domain north of  $40^\circ\text{N}$ , with temperatures ranging from  $3.2^\circ$  to  $3.4^\circ\text{C}$  and salinities ranging from 34.94 to 34.96. Mediterranean Water continues to dominate the basin interior, although the contrast between the property characteristics of the tongue at the eastern boundary and those at the western boundary is much reduced from the surfaces above; there is only a  $1^\circ\text{C}$  (0.2) difference in the temperature (salinity) of these waters from boundary to boundary. One notable difference from the 32.35 surface is the reduction in the northern extent of the Mediterranean tongue. Meridional synoptic sections in this area confirm the sharpness of the transition between the cold and fresh northern waters and the warm and salty Mediterranean waters (AHRAN, COLIN DE

VERDIERE and MEMERY, 1994). MCCARTNEY (1992) attributes this compression of the Mediterranean tongue to the presence of a deep cyclonic gyre over the West European basin. Finally, the third water mass on this surface is the cold and fresh water (3.3° to 3.4°C and 34.96 to 34.98) that stems from the equator in two branches; one to the east of the Mid-Atlantic Ridge and one to the west. The relatively high salinity of the western branch suggests that it is a combination of South Atlantic water and recirculated DWBC (RICHARDSON and SCHMITZ, 1993).

*Circulation: Fig. 17*

For the interpretation of flow on this surface we assume the same reference levels as for the preceding surface: a deep level-of-no-motion is assumed for the subtropical circulation, including the Gulf Stream and its extension into the NAC. A reference level shallower than this surface is assumed for the DWBC, the tropics and the eastern basin and a mid-depth level of minimum speed is used for the subpolar region. The Gulf Stream and North Atlantic Current on this surface are structurally similar to the preceding surface, with the Gulf Stream extending around the Tail of the Grand Banks and flowing into the NAC. The intensity of pressure gradients defining the Gulf Stream and the NAC at this level is indicative of their shear signatures penetrating well below the thermocline (first recognized by WORTHINGTON, 1954; and later related to the deep flow by FUGLISTER, 1963). The lack of a clear delineation between these currents and the southward and westward-flowing DWBC reflects (once again) the arbitrary choice of reference level. Given the property distribution in the region (particularly the presence of low salinities around the Tail of the Grand Banks), we surmise that the strong shear in that locale is in part the result of the retroflexion of the DWBC south of the Grand Banks and its convergence with waters extending into the NAC from the Gulf Stream. Thus, as the NAC flows northward and then eastward (near 50°N), the warmer, salty waters of the subtropical gyre are juxtaposed to the colder, fresher waters from the subpolar gyre.

Contrary to the preceding surfaces, the subtropical waters on this surface, carried by both the Gulf Stream and the NAC, are circulated back into the subtropical gyre. Sill depths of ~1000m are a topographic barrier for flow of this density into the Nordic Seas. Strong pressure gradients offshore of both the Gulf Stream and the NAC, and an assumption of a deep reference level, signal an anticyclonic recirculation of the subtropical waters in this vicinity. This contrasts with the preceding surface which lacks a shear signature for the waters south and east of the Gulf Stream. As defined by the 2200db contour the recirculation signature extends from near 50° to 35°N and from 20° to near 75°W. The NAC then flows eastward over the Mid-Atlantic Ridge, recirculates anticyclonically southeast of Ireland and flows westward back over the ridge. It continues along the western flank of the Mid-Atlantic Ridge, turning westward near 37°N, to rejoin the Gulf Stream, thus forming a strong, extensive anticyclonic recirculation of the subtropical waters. We note again that our interpretation of this entire system is based on the use of a deep reference level. While this has been commonly used in the western part of our domain, its use east of the ridge is less substantiated. Thus, we are interpreting the strong redevelopment of the shear on this surface east of the ridge as a *plausible* signature of anticyclonic flow.

Imbedded within this large recirculation cell are four distinct local recirculations that are separated by low pressure ridges that coincide with topographic features. The New England Seamount chain separates two local recirculations along approximately 60°W, with the westernmost recirculation (in the Sargasso Sea) appearing to be a deep signature of the recirculation noted for the preceding surface. A second break in the large recirculation occurs at the southeast Newfoundland Rise, where there is a prominent saddle point in the pressure contours. The third separation occurs at 30°W along the axis of the Mid-Atlantic Ridge, where the local Newfoundland

basin gyre connects with the anticyclonic circulation east of the ridge.

Several authors have previously focused on the link between the Gulf Stream and the NAC. WORTHINGTON's (1976) scheme for the deep circulation ( $<4^{\circ}\text{C}$ ) shows anticyclonic flow in the Newfoundland basin and in the Sargasso Sea, yet he shows a complete break between these two gyres near the Tail of the Grand Banks, such that there is no flow of the deep Gulf Stream into the NAC. The works of CLARKE, HILL, REININGER and WARREN (1980), MCCARTNEY (1992) and SCHMITZ and MCCARTNEY (1993) amended this original scheme to include a link provided by the deep Gulf Stream turning northwards to supply the North Atlantic Current. MCCARTNEY's (1992) examination of synoptic dynamic height charts showed a division into two recirculation cells northeast and southwest of the Tail, with a narrow neck between them provided by the deflection of the deep Gulf Stream around the Tail of the Grand Banks. Our maps suggest a further amendment: the continuity of the *southward* flow of the northern anticyclonic flow (in the Newfoundland basin) to the *westward* return flow of the southern anticyclonic flow (in the Sargasso Sea). In this scheme Worthington's two gyres are encompassed by a larger-scale anticyclonic recirculation. Such a recirculation of the subtropical waters is supported by the fairly homogeneous distribution of water mass properties throughout this region. The possible extension of this recirculated flow into the region east of the Mid-Atlantic Ridge is a feature that has not received recent notice, but is consistent with an idea first proposed by HELLAND-HANSEN and NANSEN (1926); that the NAC east of the ridge may be influenced by the Mediterranean waters because of an anticyclonic flow at depth. Finally, we note that REID (1978) remarked on a southwestward flow in this vicinity, but that flow was associated with Mediterranean waters rather than recirculated subtropical waters, and did not include the prominent neck at  $32^{\circ}\text{W}$ .

The southern branch of the subpolar gyre is formed by the eastward-flowing NAC, carrying both subpolar and subtropical waters. The subpolar waters join the overflow waters to form the northern branch of the subpolar gyre, or Deep Northern Boundary Current (DNBC) (MCCARTNEY, 1992), which is present in our domain to the east of the Reykjanes Ridge, flowing to the southwest. (Again, with sill depths of well less than 1000m, there is no flow at this density into the Nordic Seas.) The DNBC then loops around the Reykjanes Ridge at the Charlie-Gibbs Fracture Zone ( $52^{\circ}\text{N}$ ,  $35^{\circ}\text{W}$ ) and flows to the northeast on the west side of the ridge, forming a cyclonic circulation in the Irminger basin. The DNBC then flows to the southwest along the east coast of Greenland, loops around Greenland to flow northward along Greenland's west coast, where it forms a cyclonic circulation within the Labrador basin. The western limb of the subpolar gyre, flowing southward off the coast of Labrador and Newfoundland, constitutes the DWBC. This southward-flowing DWBC (marked by the 1700-2000db contours) continues along the coast and is tracked around the Tail of the Grand Banks to approximately  $55^{\circ}\text{W}$ . We note again that the demarcation between the DWBC and the northward-flowing NAC, and the eastward-flowing Gulf Stream, remains unclear.

In summary, the circulation on this surface is markedly different than the preceding surfaces: The shallower surfaces are involved with a net export of subtropical waters to the subpolar region, the upper limb of the meridional overturning cell. As a result the subtropical gyre flow does not contain much subpolar influence. This surface, however, is deep enough to be involved with the net export of subpolar water to the subtropics. This export is initiated by westward flow along the northern boundary of the subpolar gyre which, after flowing southward as the DWBC, branches into continued deep western boundary flow in the subtropics and eastward flow in the deep North Atlantic Current. This latter branch, with its anticyclonic recirculation gyre, carries water southward into the interior of the subtropical gyre. This is part of the complex circulation whose integrated effect constitutes the lower limb of the meridional overturning cell.

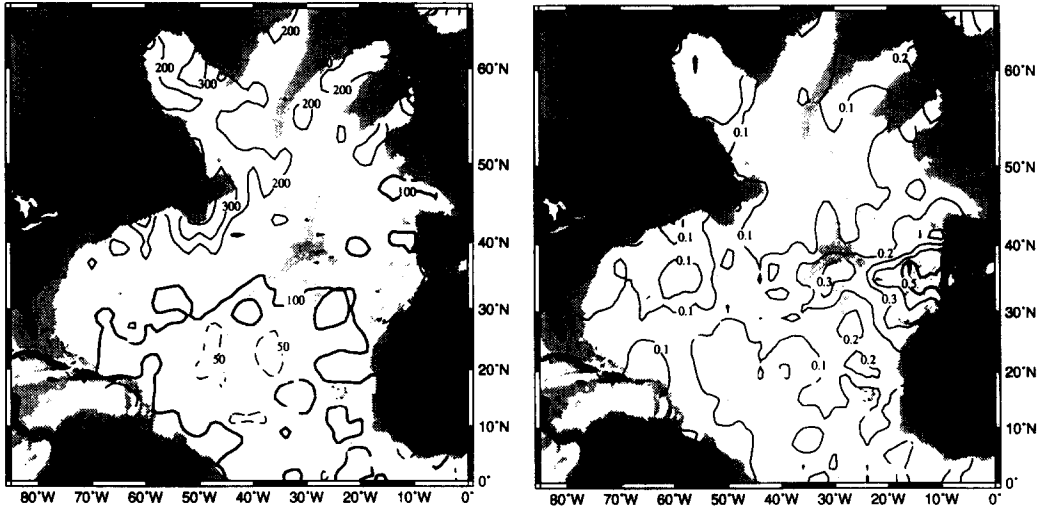
*Variability: Fig.18*

Fig.18. Standard deviation fields for the  $\sigma_2=36.95$  surface.

The variance of potential temperature for this surface shows a range from only 0.1 to 0.2°C, except for the higher values in the eastern basin that are associated with the strong gradients of the Mediterranean tongue. The variability of pressure on this surface is generally on the order of 50 to 100db, with higher values (200 to 400db) east of Labrador and in the vicinity of the Tail of the Grand Banks, similar to the previous surface.

5.6  $\sigma_3 = 41.45$  and  $41.50$

*Water properties: Figs 19 and 21*

These surfaces, both below 3°C, are generally below the depth of Labrador Sea Water, and are instead mainly characterized by overflow waters in the north, North Atlantic Deep Water, Lower Deep Water (LDW) (MCCARTNEY, 1992) and Mediterranean water in the mid and lower latitudes. On both surfaces the influence of the Norwegian Sea overflow waters is evident from the high salinity and temperature contours wrapped around the Reykjanes Ridge. The relatively cooler and fresher waters from the Denmark Strait are seen along the eastern coast of Greenland to the Newfoundland basin. On the 41.45 surface, the warm and salty Mediterranean waters, extending across the midbasin to nearly 70°W act as a wedge between LDW to its south and NADW to its north. Thus, for this shallower surface the cold and fresh LDW from the southern portion of the domain does not appear to penetrate north of 20°N. In contrast, the 41.50 temperature and salinity fields show only a remnant of the warm and saline Mediterranean tongue near the eastern boundary: the tongue on this surface is geographically confined to east of 20°W and has little direct influence north of 40°N. Thus, it appears that this deeper surface is dominated mainly by LDW and NADW.

Because the 41.50 surface (at approximately 2.4°C) lies near where there is a minimum range in the  $\theta$ -S relation for the North Atlantic (WRIGHT and WORTHINGTON, 1970; WORTHINGTON and WRIGHT, 1970), the contrast between LDW and NADW is not pronounced on this surface. Nonetheless, the northward penetration of LDW, described in detail by MCCARTNEY (1992), is

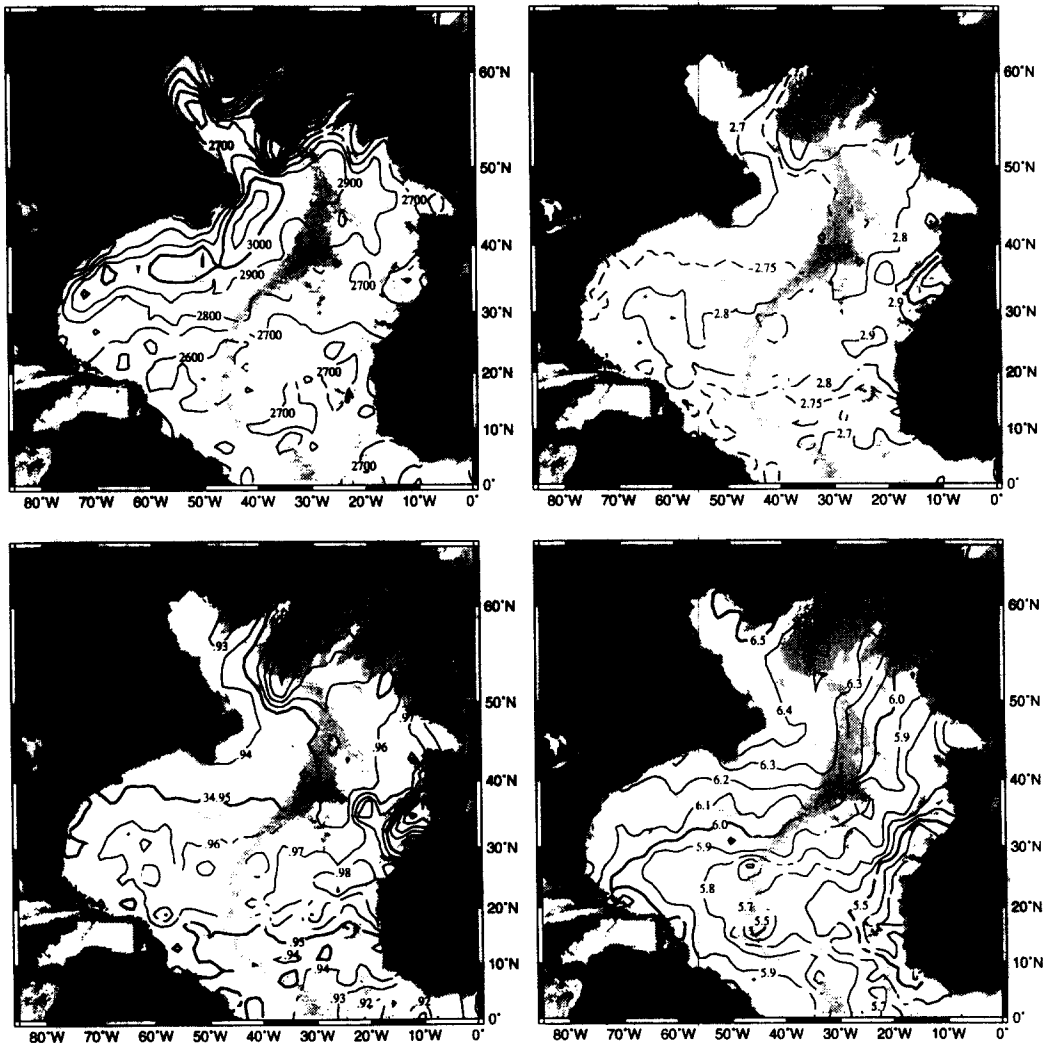


Fig. 19. Mean properties for the  $\sigma_3=41.45$  surface. Light gray shading delineates bathymetry  $<3000\text{m}$  and darker gray is  $<2000\text{m}$  on all 41.45 maps.

evident in both the western and eastern basins on the 41.50 surface from the salinity and oxygen maps. The signature of LDW (low salinity and low oxygen) is seen to extend in the western basin to nearly  $30\text{--}35^\circ\text{N}$ , in accordance with MCCARTNEY's (1992) description of the LDW signal fading at the southern edge of the deep Gulf Stream recirculation. The 41.50 oxygen field shows this delineation between the NADW and the LDW in the western basin and also suggests a convergence of the LDW (marked by the 5.9 and 6.0 contours) into the southward-flowing DWBC near  $30^\circ\text{N}$  (MCCARTNEY, 1992). These relatively low oxygen values contrast with the high oxygens of the NADW carried southward by the DWBC, with the southward penetration of the 6.1 contour marking the DWBC route along the western North America coast. The penetration of LDW into the eastern basin on the 41.50 surface is marked by the zonal alignment of the oxygen contours in the vicinity of the Vema Fracture Zone, in agreement with the work of MCCARTNEY, BENNETT and

WOODGATE-JONES (1991). The salinity and oxygen fields show a general trend for the northward flow of LDW to shift from the eastern flank of the Mid-Atlantic Ridge to the northern European coast. The shift occurs in the region bounded by 30°-40°N, in agreement with MCCARTNEY, BENNETT and WOODGATE-JONES (1991) and SAUNDERS (1987). The LDW in the northern portion of the eastern basin is marked by the low saline (~34.93) waters that contrast with the saltier NADW and Mediterranean waters. Finally, we note that the low oxygens off the northwest coast of Africa appear at these deep surfaces also, yet here their signal is weaker and more geographically-confined, particularly so for the 41.50 surface.

*Circulation: Figs 19 and 21*

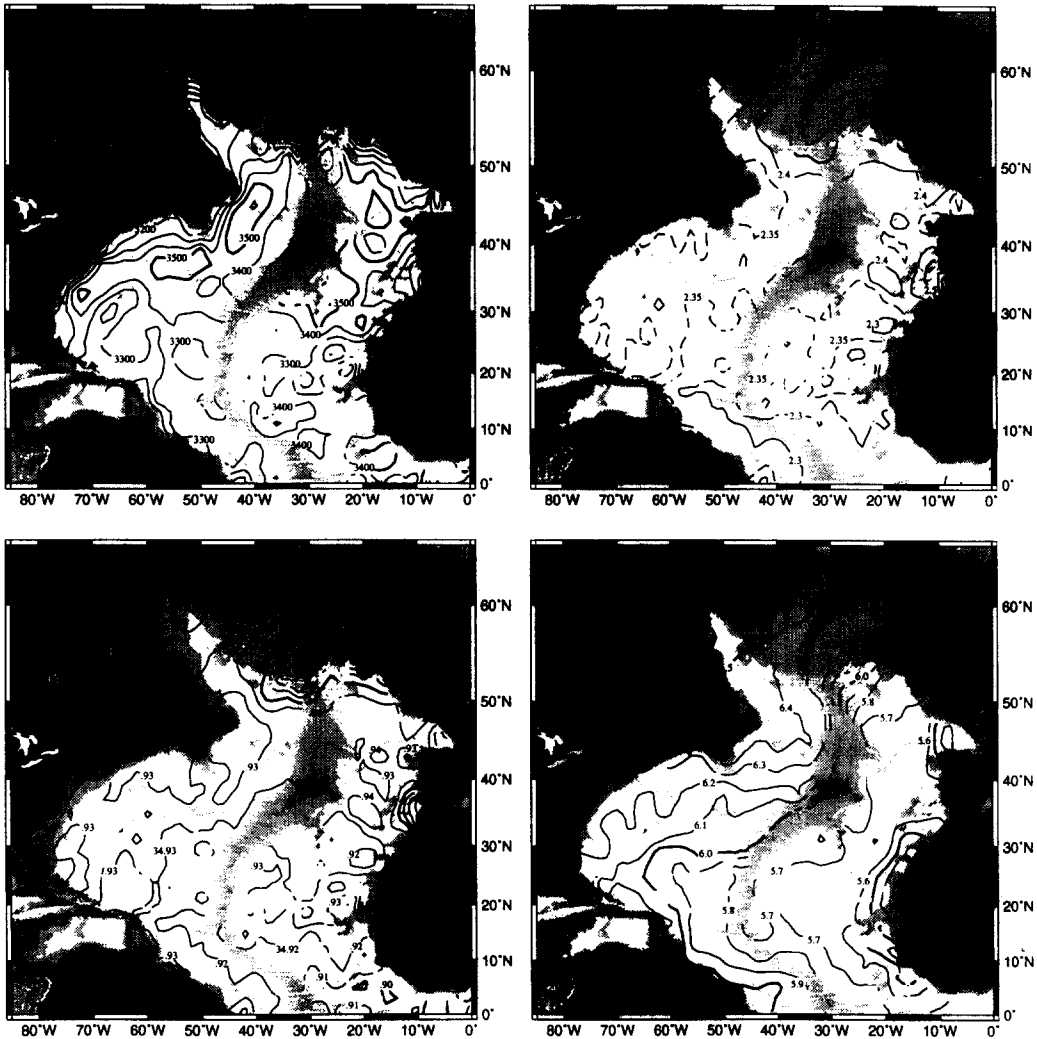


Fig.21. Mean properties for the  $\sigma_3 = 41.50$  surface. Light gray shading delineates bathymetry  $< 3500\text{m}$  and darker gray is  $< 2000\text{m}$  on all 41.50 maps.

On these surfaces the recirculation of the subtropical waters carried by the deep Gulf Stream and NAC is again evident in the pressure field. The recirculation on these deeper surfaces is restricted to the western side of the Mid-Atlantic Ridge, where there is a southwestern closure. The anticyclonic recirculation, as with the 36.95 surface, is comprised of smaller-scale recirculations, with the Newfoundland basin recirculation and the recirculation east of the New England Seamounts appearing on these surfaces. The shear signature for the subpolar gyre is strong on these deep surfaces, particularly the shear associated with the DNBC as it loops around both the Reykjanes Ridge and Greenland. Structurally, the subpolar gyre is similar to that described for the 36.95 surface, with a notable exception. At the depth of the 41.50 surface the northern waters are joined at these latitudes by the LDW that has travelled northward within the eastern basin. Thus, in accordance with MCCARTNEY (1992), the 3400 and 3500db contours in the eastern basin are interpreted as the northeastward flow carrying LDW (as evidenced in the property fields for these surfaces). This current joins the Iceland Faroe Overflow in the Iceland Basin, with both flowing westward through the Gibbs Fracture Zone. This branch constitutes the main “recirculating components to the deep boundary current of the northern North Atlantic” of MCCARTNEY (1992). After the Gibbs Fracture Zone, this branch splits between a northward branch that loops through the Labrador basin and one that flows more directly into the DWBC, just northeast of the Flemish Cap. The division at the Gibbs Fracture Zone between an eastward-flowing NAC and this westward-flowing branch is, of course, unclear, and must be reconciled with ancillary information. Finally, on the 41.50 surface the signature of the southward-flowing DWBC is particularly strong around the Tail of the Grand Banks and east of the US coast. The signature of the DWBC is also apparent off the northern coast of South America (near 10°-15°N), with a zonal extension (marked by the 3300-3100db contours) near 3°N.

*Variability: Figs 20 and 22*

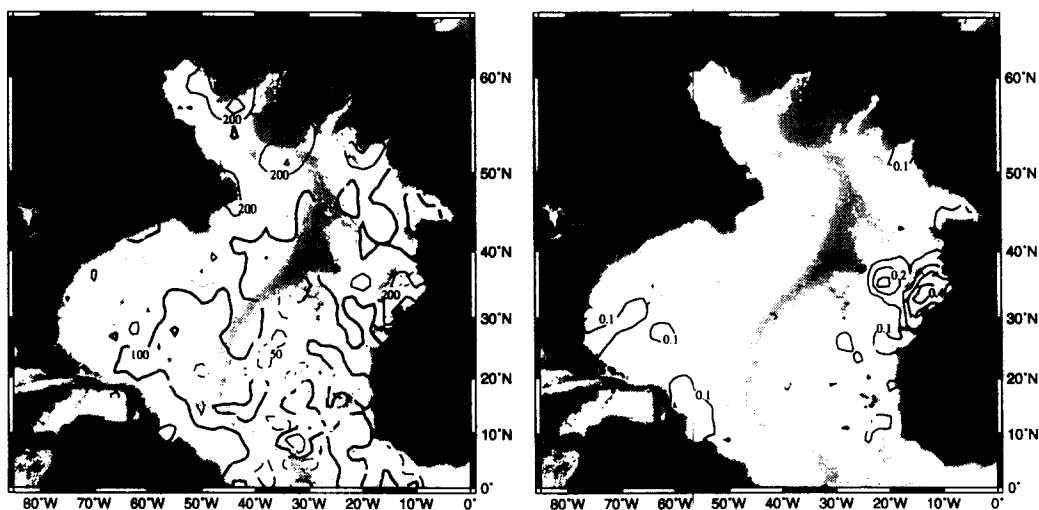


Fig.20. Standard deviation fields for the  $\sigma_3=41.45$  surface.

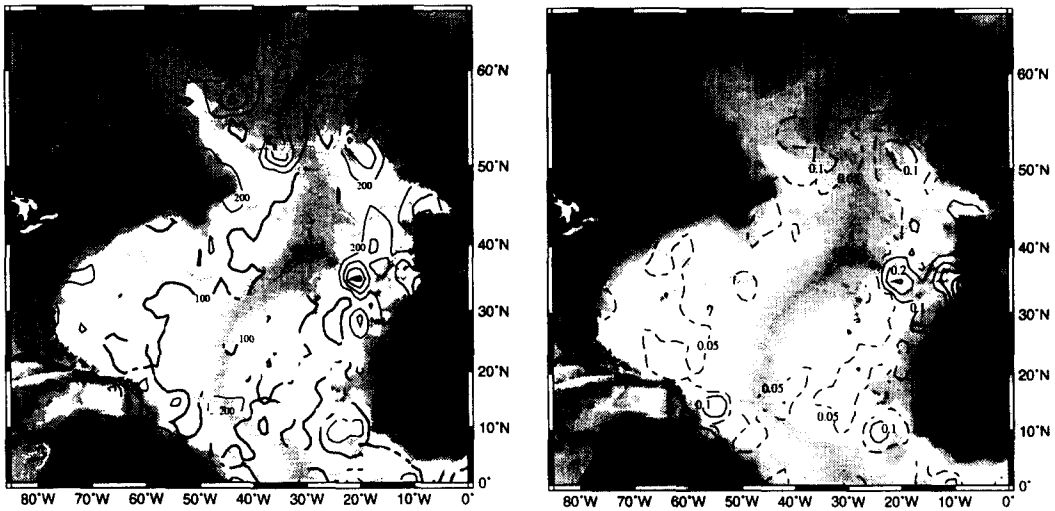


Fig.22. Standard deviation fields for the  $\sigma_3=41.50$  surface.

Temperature standard deviations are generally  $0.1^\circ\text{C}$  for the 41.45 surface and  $0.05^\circ\text{C}$  for the 41.50 surface. Elevated values are restricted almost entirely to the region of the Mediterranean tongue on these surfaces, with values typically  $0.2^\circ\text{C}$  in this locale. The standard deviation for the pressure field is marked by values generally less than 100db in the domain south of  $50^\circ\text{N}$  and east of  $50^\circ\text{W}$ . Elsewhere values range from 100 to 200db.

5.7  $\sigma_4 = 45.90$

#### *Water properties: Fig 23*

Because this surface is characterized by  $1.8^\circ\text{C}$  water, it lies at the division between what SCHMITZ and MCCARTNEY (1993) term deep water ( $1.8^\circ$  to  $4.0^\circ\text{C}$ ) and bottom water ( $<1.8^\circ\text{C}$ ). At the level of the bottom waters in the North Atlantic there is a fundamental change in the source waters into this basin. While NADW continues to be the important northern source, there is now a substantial southern source for these bottom waters, such that there is a *net* mass inflow into the North Atlantic at these depths. Thus, the waters are forced to upwell into the overlying layer. This has a direct bearing on the interpretation of the 45.90 maps because the upwelling waters directly affect the properties and flow on this surface. In addition to this advective influence, it is recognized that vertical diffusive fluxes are important at these depths because abyssal vertical property gradients exceed horizontal property gradients. Thus, our two-dimensional maps are incomplete for the visualization of the complete advective-diffusive flow pattern and must be supplemented with a view of the vertical mixing and advective pathways.

This surface appears almost exclusively on the western side of the Mid-Atlantic Ridge. Only the southern end of the eastern basin contains water of this density, which has apparently entered through the Vema Fracture Zone, supplying the abyss north of the Sierra Leone Rise. The temperature, salinity, and oxygen ranges on this abyssal surface are  $0.2^\circ\text{C}$ , 0.05 and  $1.0\text{ml l}^{-1}$ , respectively. In spite of these small ranges two water masses are distinct: North Atlantic Deep Water (NADW) and Antarctic Bottom Water (AABW). Initially cold and fresh ( $<1.8^\circ\text{C}$  and

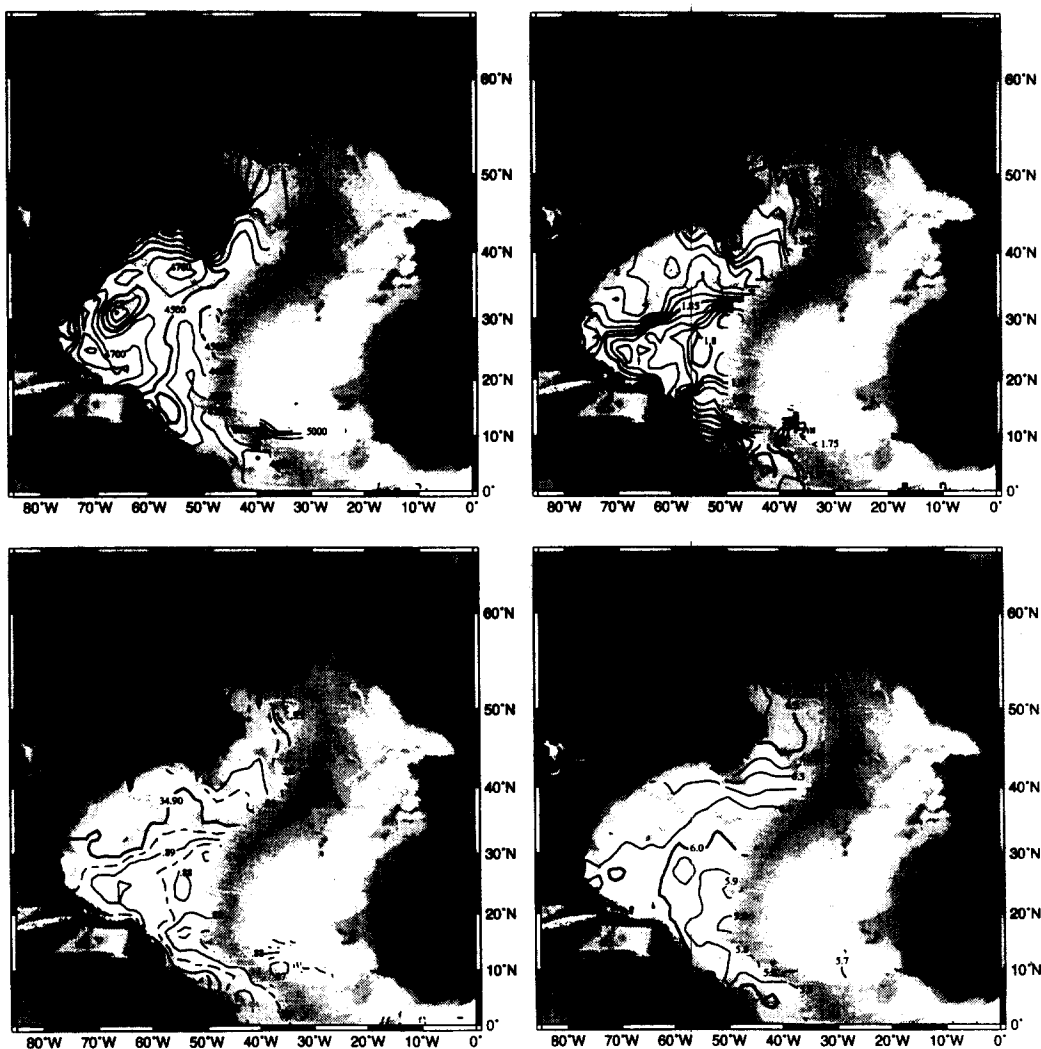


Fig.23. Mean properties for the  $\sigma_t=45.90$  surface. Gray shading delineates successive bathymetric contours of 4500, 4000, 3000 and 2000m on all 45.90 maps.

<34.88), the AABW flows northward across the equator and continues along the western flank of the Mid-Atlantic Ridge, warming and increasing in salinity along its path. These changes in AABW properties along its path are attributed to mixing with the overlying warmer and saltier NADW (LUYTEN, MCCARTNEY and STOMMEL, 1993).

Although the temperature and salinity fields in the northern domain show a clear signal of NADW, the most distinct signal is in the oxygen field. The high oxygens in the north, characterizing newly formed waters, are seen to extend southward along the western boundary to approximately 10°N. Such a strong signal is attributed to the advection of the DWBC, with the attendant decrease in oxygen values resulting primarily from entrainment of lower oxygen values along its path. A simple picture of the water masses on this surface is one of the NADW occupying the region north of 34°N and penetrating to the south along the western boundary, with the AABW occupying the

southern domain and filling the eastern portion of the western basin up to the approximate location of the Gulf Stream. As a rough guide to the delineation of these two water masses it can be supposed that the  $6.0 \text{ ml l}^{-1}$  oxygen contour divides the NADW from the AABW.

*Circulation: Fig.23*

The circulation for this surface is interpreted with a shallow reference level for the entire domain. On the western flank of the Mid-Atlantic Ridge a northward flow of AABW is indicated by the (generally) meridional orientation of the 4300-4500db contours, in agreement with SPEER and MCCARTNEY (1992). The northern penetration of this water mass is supported also by the signatures of AABW in the temperature, salinity and oxygen fields, as noted above. Based on the work of SCHMITZ and MCCARTNEY (1993) and TUCHOLKE, WRIGHT and HOLLISTER (1973), on our maps a second branch of the northward-flowing AABW emerges from the Puerto Rico Trench, flowing eastward and then northward (marked by the path of the 4500-4700db contours north of Puerto Rico). Following this northward flow, our fields suggest that the AABW then flows southwestward around Bermuda, in agreement with the scheme proposed by SCHMITZ and MCCARTNEY (1993). The flow (marked by the 4500-4700db contours) continues to the north and west of Bermuda and joins the DWBC (to be discussed next) as a southwestward flow near  $35^{\circ}\text{N}$ . This potential flow path for the recirculation of AABW is supported by the isobars on our pressure map that show a strong anticyclonic gyre centered on the Bermuda Rise. This anticyclonic flow is partially verified by direct velocity measurements that show strong southwestward flow along the southeastern flank of the Bermuda Rise (BIRD, WEATHERLY and WIMBUSH, 1982) and an eastward flow on the northern side (OWENS, LUYTEN and BRYDEN, 1982).

There is no appreciable shear associated with either a deep Gulf Stream or NAC for this abyssal surface. The strong shear signature along the western boundary is to the north and east of the Gulf Stream and NAC noted on the shallower surfaces, and is instead interpreted as a signature of the DWBC (ARMI and WILLIAMS, 1991; MCCARTNEY, 1992; WEATHERLY and KELLY, 1985). As the DWBC flows southward off the Labrador and Newfoundland coasts there are apparent convergences into this current, marked by the 3600 to 4400db contours. After the DWBC flows around the Tail of the Grand Banks, there is a cyclonic recirculation (marked by the 4700db bowl of pressure) associated with the current (HOGG, PICKART, HENDRY and SMETHIE, 1986). At approximately  $35^{\circ}\text{N}$  over the Hatteras Abyssal Plain, there is a convergence into the DWBC of a southwestward flow comprised mainly of AABW, as noted above. The Blake Bahama Outer Ridge deflects the DWBC seaward such that it misses Abaco (AMOS, GORDON and SCHNEIDER, 1971). An abyssal shelf keeps the DWBC offshore until approximately  $23^{\circ}\text{N}$ . South of this locale the DWBC is not resolved.

Finally, of note on this surface is the zonal orientation of the isobars near  $10^{\circ}\text{N}$ . This pattern, with a shallow reference level, is suggestive of an eastward abyssal jet feeding water through the Vema Fracture Zone (SPEER and MCCARTNEY, 1992; KAWASE, 1993). Because this surface does not appear on the eastern side of the ridge (except for the partial cyclonic gyre evident over the Gambia Abyssal Plain) the waters are apparently warmed and/or freshened as they cross the ridge (MCCARTNEY, BENNETT and WOODGATE-JONES, 1991). MCCARTNEY and CURRY (1993) estimate the supply of AABW to the western North Atlantic at  $4\text{Sv}$ , and SCHMITZ and MCCARTNEY (1993) indicate about half of this is diverted by the eastward flow through the Vema Fracture Zone. The  $2\text{Sv}$  that continues northward is indicated in their charts as a net flow achieved as a difference between opposing limbs of a strong cyclonic gyre north of  $10^{\circ}\text{N}$ , which appears in our pressure map with the isolated pressure maximum  $>4500\text{db}$  in the Guiana Abyssal Plain. KAWASE's (1993) modelling efforts have produced such a gyre as a response to northward deepening topography.

Variability: Fig.24

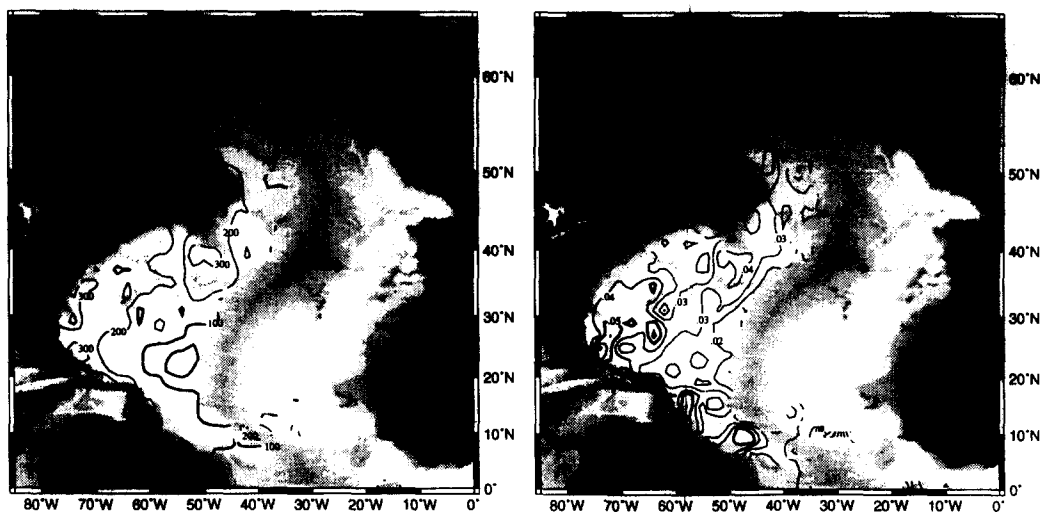


Fig.24. Standard deviation fields for the  $\sigma_4=45.90$  surface.

The standard deviation fields for each of the water properties are relatively flat. Consistent with the uniformity of the temperature and salinity at this depth the standard deviations are only  $\sim 0.04^\circ\text{C}$  and 0.01, respectively. There is no distinction in the variability between the NADW and AABW waters for temperature or salinity. For the pressure field in the northern domain the standard deviation is approximately 200db, with pockets of higher variability near the Blake Bahama Outer Ridge, around the Tail of the Grand Banks, and north of Puerto Rico. Generally, higher variabilities occur in the northern and western part of our domain. Since the surface is very close to the bottom in these locales, perhaps its stronger variability can be attributed to the influence of the small scale topography on this steeply-tilted density surface.

## 6. COMPARISON WITH LEVITUS FIELDS

The property fields from our database were compared to the LEVITUS (1994) property fields (after a projection of the two databases onto common isopycnals) in order to assess the differences. To summarize the comparison, the mean pressure and temperature derived from the Levitus data set for the surfaces,  $\sigma_0 = 27.00$  and  $\sigma_4 = 45.90$ , are shown in Fig.25. An examination of the Levitus pressure field for the  $\sigma_0 = 27.00$  surface and the pressure field depicted in Fig.10 shows that the Levitus field has a considerably broader Gulf Stream, the curvature of the isobars at the Tail of the Grand Banks is much reduced in the Levitus field and the retroflexion of the NAC is much more pronounced in the field from our database. These differences are easily attributed to the resolution differences between the two databases.

The Levitus potential temperature field also exhibits larger smoothing when compared to the potential temperature field (Fig.10) from our database (e.g. the gradient in the Labrador Sea is much more defined in our field.) Additionally, there is a notable difference in these two fields. Prominent in the Levitus field, but absent in our field, is an isolated lozenge of warm water that extends from Cape Hatteras to approximately  $50^\circ\text{W}$ , straddling the mean path of the Gulf Stream. The  $14.0^\circ\text{C}$  water in this isolated lozenge contrasts sharply with the  $12.2^\circ\text{C}$  water found in our field

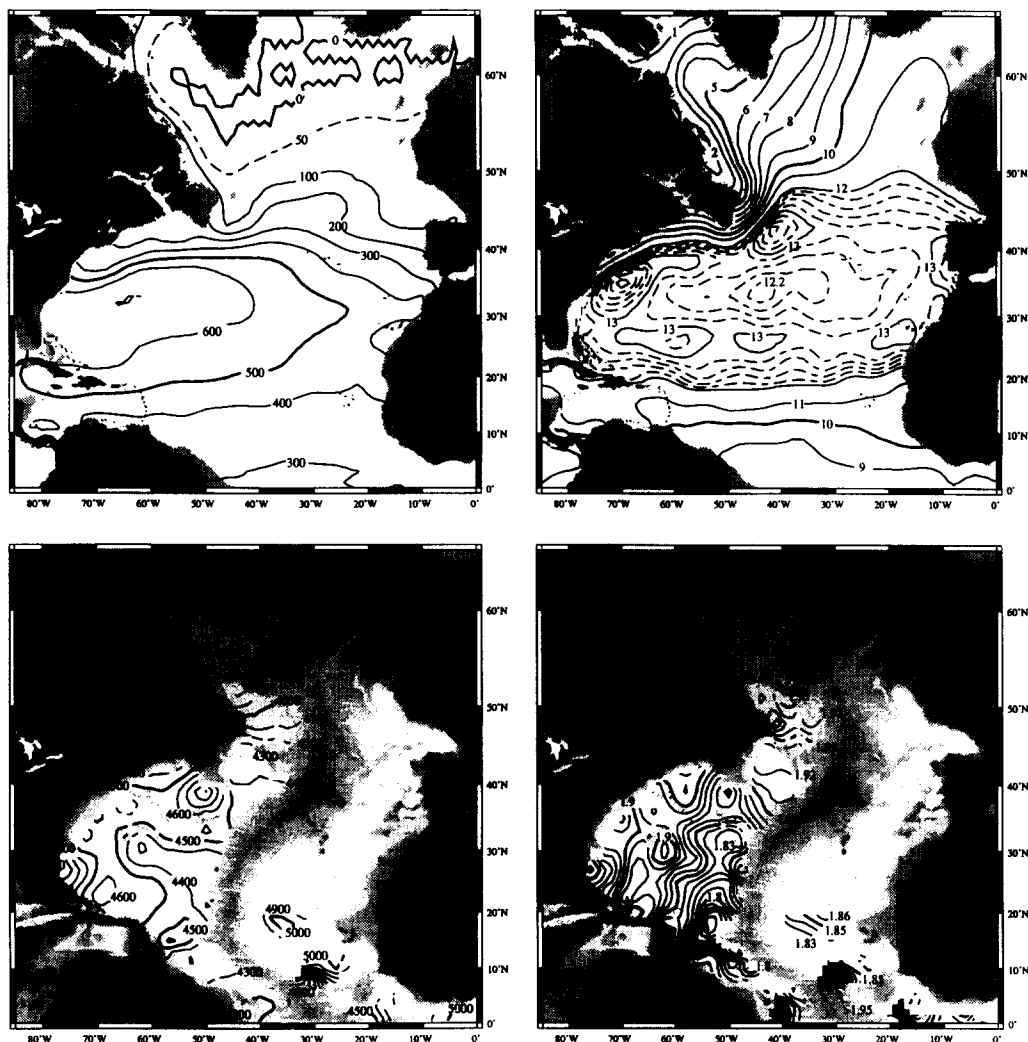


Fig.25. Property maps compiled from the LEVITUS (1994) data set.

at the same locale. Not only is this water decidedly cooler, but there is no hint of closed isotherms in that vicinity for our field. A difference is also found in the Levitus salinity field (not shown): a salty lozenge appears with salinities considerably larger than those found in our database. A similar warm lozenge appears on the southern flank of the Gulf Stream/NAC system just south of the Newfoundland basin, and two are evident at the southern edge of the subtropical gyre. Additionally, a cold lozenge appears in the centre of the gyre, with temperatures approximately  $0.4^{\circ}\text{C}$  cooler than those in our map. While the other differences on this surface can be accounted for by the difference in the smoothing scales between the two databases these differences in water mass characteristics cannot be similarly explained. Instead, LOZIER, MCCARTNEY and OWENS (1994) have shown that these differences result from anomalies that are introduced when climatological data are averaged on isobars rather than isopycnals. Basically, when data are averaged and smoothed on isobars an artificial mixing is introduced in the vicinity of sloping isopycnals which

produces water mass characteristics dissimilar to those of the surrounding synoptic water masses. The warm anomalies are a product of isobaric-averaging in the vicinity of unidirectionally-sloping isopycnals while the cold anomaly is a product of isobaric-averaging in the vicinity of an isopycnal bowl (i.e. the centre of the subtropical gyre). Further details are given in LOZIER, MCCARTNEY and OWENS (1994).

The difference between our potential temperature field for the  $\sigma_4 = 45.90$  surface (Fig. 23) and Levitus' is mainly one of resolution north of  $40^\circ\text{N}$ . South of  $40^\circ\text{N}$ , where the fields are similarly resolved, the temperatures are in agreement in terms of magnitude, yet there are differences in the structure of the two temperature fields. Most notable of these differences is the zonal band of contours ( $1.82^\circ$ - $1.87^\circ\text{C}$ ), roughly along  $33^\circ\text{N}$ , that marks a transition between waters of northern and southern origin in our map. In the Levitus map the boundary between these waters appears to be oriented meridionally, along approximately  $60^\circ\text{W}$ . In the pressure fields for this surface the resolution differences are large enough that the Levitus field north of  $40^\circ\text{N}$  gives only a glimpse of the structure evident from our mean pressure field. South of this latitude, the anticyclonic gyre seen near Bermuda in our database is not resolved in the Levitus field. The most important difference, however, is the resolution of the DWBC in our map. This resolution not only depicts the continuity of the DWBC, but it also gives a clearer picture as to how the recirculations are associated with this boundary current.

## 7. SUMMARY

A new database has been assembled for the North Atlantic from the station data stored in the archives of the National Oceanographic Data Centre. Approximately 144,000 stations were available from the period 1904 to 1990. A series of quality control checks on the station data reduced the data set by 9%. The sanitized data were then averaged and smoothed to produce a one-degree gridded database of mean pressures, temperatures, salinities and oxygens on selected isopycnals. This analysis differs significantly from Levitus' in that the resolution has been increased by an order of magnitude and that the averaging of the properties has been done on isopycnals rather than on isobars. The latter choice introduces artificial water mass anomalies in the vicinity of sloping isopycnals.

Overall, this database more finely resolves the major features of the North Atlantic that have been studied extensively, namely the Gulf Stream, the North Atlantic Current, the Azores Current and the Deep Western Boundary Current. A simple comparison with the Levitus fields indicates the degree of improvement in the resolution of these currents and their associated property fields. Additionally, the database illuminates the baroclinicity of these major currents and elucidates the recirculations associated with them. In this regard the database has revealed features that were not evident from the Levitus database. In general these features are located at mid-ocean depths or in the abyss where the relatively high resolution of this database is most needed because of the decreasing scale of the circulation with depth. But perhaps the contributions of the database should not be judged solely in terms of its improvement over the Levitus atlas, but rather in terms of how it matches numerous synoptic features. As noted throughout the text, this database reveals a composite of North Atlantic circulation and property features that have been observed from synoptic studies, but have not yet appeared in a climatological database.

A new feature which has emerged from this analysis is the signature of a large scale recirculation on the subtropical waters from the eastward extension of the North Atlantic Current. The recirculation occupies the central domain of the basin and encompasses the more local recirculations associated with both the Sargasso Sea waters and those of the Newfoundland Basin. This gyre, with

similar pattern and extent, is found on surfaces from near 1800db to 3600db. The recirculation potentially carries waters of subtropical origin that have been in direct contact with subpolar waters back into the subtropical gyre. Additionally, this database provides a basin view of the Azores Current. Our maps reveal a continuity of southeastward flow from the region south of the Tail of the Grand Banks (where it branches from the Gulf Stream system) to the eastern boundary near Madeira. The current is marked by strong divergences to the south and by convergences from the north. The diverging waters return to the subtropical gyre and converging waters stem from the North Atlantic Current.

Future work with this database includes the extension of our domain to include the South Atlantic and the northern North Atlantic. Additionally, the database will be used to examine the decadal and/or interannual variability of the Atlantic basin. Readers interested in this database should send requests to [hydrobase@whoi.edu](mailto:hydrobase@whoi.edu) or [susan@neptune.geo.duke.edu](mailto:susan@neptune.geo.duke.edu).

## 8. ACKNOWLEDGEMENTS

The authors wish to thank N. Hogg for his role in the initiation of this work. Additionally, the authors thank M. McCartney for his insightful discussions and invaluable suggestions. The comments of B. Pickart and an anonymous reviewer were extremely helpful in the revision of this manuscript. Support from the National Science Foundation, Grant OCE-9103364, for the authors is gratefully acknowledged as is the support from the National Oceanic and Atmospheric Administration, Grant NA36GP0137-01 for RGC.

## 9. REFERENCES

- AHRAN, M. (1990) The North Atlantic Current and Subarctic Intermediate Water. *Journal of Marine Research*, **48**, 109-144.
- AHRAN, M., A. COLIN DE VERDIERE and L. MEMERY (1994) The eastern boundary of the Subtropical North Atlantic. *Journal of Physical Oceanography*, **24**, 1295-1316.
- AMOS, A.F., A.L. GORDON and E.D. SCHNEIDER (1971) Water masses and circulation patterns in the region of the Blake-Bahama Outer Ridge. *Deep-Sea Research*, **18**, 145-165.
- ARMI, L. and R. WILLIAMS (1991) The deep western boundary undercurrent off the Newfoundland Ridge. *Deep-Sea Research*, **38**, 371-391.
- ARMI, L. and W. ZENK (1985) Large lenses of highly saline Mediterranean Water. *Journal of Physical Oceanography*, **14**, 1560-1576.
- BIRD, A.A., G.L. WEATHERLY and M. WIMBUSH (1982) A study of the bottom boundary layer over the eastward scarp of the Bermuda Rise. *Journal of Geophysical Research*, **87**, 7941-7954.
- CLARKE, R.A., H.W. HILL, R.F. REININGER and B.A. WARREN (1980) Current system south and east of the Grand Banks of Newfoundland. *Journal of Physical Oceanography*, **10**, 25-65.
- CORNILLON, P. (1986) The effect of the New England Seamounts on Gulf Stream meandering as observed from satellite imagery. *Journal of Physical Oceanography*, **15**, 386-389.
- DIETRICH, G., K. KALLE, W. KRAUSS and G. SIEDLER (1975) *General Oceanography*. John Wiley, 626pp.
- FUGLISTER, F.C. (1960) *Atlantic Ocean Atlas*. Woods Hole Oceanographic Institution, Woods Hole, 209pp.
- FUGLISTER, F.C. (1963) Gulf Stream '60. *Progress in Oceanography*, **1**, 265-373.
- HELLAND-HANSEN, B. and F. NANSEN (1926) The eastern North Atlantic. *Geofysiske Publikasjoner*, **4**(2), 76pp.
- HOGG, N.G. (1987) A least-squares fit of the advective-diffusive equations to Levitus Atlas data. *Journal of Marine Research*, **45**, 347-375.
- IVERS, W.D. (1975) *The deep circulation in the northern North Atlantic with special reference to the Labrador Sea*. PhD Thesis, University of California, San Diego, 179pp.
- KAWASE, M. (1993) Topographic effects on the bottom water circulation of the western tropical North Atlantic Ocean. *Deep-Sea Research*, **40**, 1259-1283.
- KLEIN, B. and G. SIEDLER (1989) On the origin of the Azores Current. *Journal of Geophysical Research*, **94**, 6159-6168.

- KRAUSS, W. (1986) The North Atlantic Current. *Journal of Geophysical Research*, **91**, 5061-5074.
- KRAUSS, W., R.H. KASE and H. HINRICHSSEN (1990) The branching of the Gulf Stream southeast of the Grand Banks. *Journal of Geophysical Research*, **95**, 13,089-13,103.
- KREYSZIG, E. (1979) *Advanced Engineering Mathematics*, John Wiley, 939pp.
- LEE, T. (1994) *Variability of the Gulf Stream path observed from satellite images*. PhD Thesis, University of Rhode Island, 188pp.
- LEVITUS, S. (1982) Climatological atlas of the world ocean. *NOAA Professional Paper*, **13**, US Government Printing Office, Washington, DC, 173pp.
- LEVITUS, S. (1994) World Ocean Atlas 1994 CD-Rom Sets. *National Oceanographic Data Center Informal Report*, **13**.
- LOZIER, M.S., M.S. MCCARTNEY and W.B. OWENS (1994) Anomalous anomalies in averaged hydrographic data. *Journal of Physical Oceanography*, **24**, 2624-2638.
- LUYTEN, J., M. MCCARTNEY and H. STOMMEL (1993) On the sources of North Atlantic Deep Water. *Journal of Physical Oceanography*, **123**, 1885-1892.
- MANN, C.R. (1967) The termination of the Gulf Stream and the beginning of the North Atlantic Current. *Deep-Sea Research*, **14**, 337-359.
- MCCARTNEY, M.S. (1982) The subtropical recirculation of Mode Water. *Journal of Marine Research*, **40** (Supplement), 427-464.
- MCCARTNEY, M.S. (1992) Recirculating components to the deep boundary current of the northern North Atlantic. *Progress in Oceanography*, **29**, 283-383.
- MCCARTNEY, M.S. (1993) The crossing of the equator by the deep western boundary current in the western Atlantic Ocean. *Journal of Physical Oceanography*, **13**, 1953-1974.
- MCCARTNEY, M.S. and R. CURRY (1993) Trans-equatorial flow of Antarctic bottom water in the Western Atlantic Ocean. *Journal of Physical Oceanography*, **23**, 1264-1276.
- MCCARTNEY, M.S. and L.D. TALLEY (1982) The subpolar mode water of the North Atlantic Ocean. *Journal of Physical Oceanography*, **12**, 1169-1188.
- MCCARTNEY, M.S. and L.D. TALLEY (1984) Warm-to-cold water conversion in the northern North Atlantic. *Journal of Physical Oceanography*, **14**, 922-935.
- MCCARTNEY, M.S., S.L. BENNETT and M.E. WOODGATE-JONES (1991) Eastward flow through the Mid-Atlantic Ridge at 11°N and its influence on the abyss of the eastern basin. *Journal of Physical Oceanography*, **21**, 1089-1121.
- MCDUGALL, T.J. (1987) Neutral surfaces. *Journal of Physical Oceanography*, **17**, 1950-1964.
- MOLINARI, R.L., R.A. FINE and E. JOHNS (1992) The Deep Western Boundary Current in the tropical North Atlantic Ocean. *Deep-Sea Research*, **39**, 1967-1985.
- MONTGOMERY, R.B. (1937) A suggested method for representing gradient flow in isentropic surfaces. *Bulletin of the American Meteorological Society*, **18**, 210-211.
- OWENS, W.B., J.R. LUYTEN and H.L. BRYDEN (1982) Moored velocity measurements on the edge of the Gulf Stream recirculation. *Journal of Marine Research*, **40** (Supplement), 509-524.
- PINGREE, R.D. and B. LECANN (1993) A shallow Meddie (a Smeddie) from the secondary Mediterranean salinity maximum. *Journal of Geophysical Research*, **98**, 20,169-20,185.
- REID, J.L. (1978) On the middepth circulation and salinity field in the North Atlantic Ocean. *Journal of Geophysical Research*, **83**, 5063-5067.
- REID, J.L. (1994) On the total geostrophic circulation of the North Atlantic Ocean: Flow patterns, tracers and transports. *Progress in Oceanography*, **33**, 1-92.
- RICHARDSON, P.L., M.S. MCCARTNEY and C. MAILLARD (1991) A search for meddies in historical data. *Dynamics of Atmospheres and Oceans*, **15**, 241-265.
- RICHARDSON, P.R. and W.J. SCHMITZ, Jr. (1993) Deep cross-equatorial flow in the Atlantic measured with SOFAR floats. *Journal of Geophysical Research*, **98**, 8371-8387.
- SAUNDERS, P.M. (1982) Circulation in the eastern North Atlantic. *Journal of Marine Research*, **40** (Supplement), 641-657.
- SAUNDERS, P.M. (1987) Flow through Discovery Gap. *Journal of Physical Oceanography*, **17**, 631-643.
- SCHMITT, R.W. and D.T. GEORGI (1982) Finestructure and microstructure in the North Atlantic Current. *Journal of Marine Research*, **40** (Supplement), 659-705.
- SCHMITZ, W.J. (1980) Weakly depth dependent segments of the North Atlantic circulation. *Journal of Marine Research*, **38**, 111-133.

- 
- SCHMITZ, W.J. and M.S. MCCARTNEY (1993) On the North Atlantic Circulation. *Reviews of Geophysics*, **31**(1), 29-49.
- SCHMITZ, W.J. and P.L. RICHARDSON (1991) On the sources of the Florida Current. *Deep-Sea Research*, **38**, Supplement 1, 379-409.
- SIEDLER, G., A. KUHL and W. ZENK (1987) The Madeira Mode Water. *Journal of Physical Oceanography*, **17**, 1561-1570.
- SMITH, W.H.F. and P. WESSEL (1990) Gridding with continuous curvature splines in tension. *Geophysics*, **55**, 293-305.
- SPEER, K.G. and M.S. MCCARTNEY (1991) Tracing lower North Atlantic Deep Water across the equator. *Journal of Geophysical Research*, **96**, 20,433-20,448.
- SPEER, K.G. and M.S. MCCARTNEY (1992) Bottom water circulation in the Western North Atlantic. *Journal of Physical Oceanography*, **22**, 83-92.
- STRAMMA, L. and G. SIEDLER (1988) Seasonal changes in the North Atlantic subtropical gyre. *Journal of Geophysical Research*, **93**, 8111-8118.
- SY, A. (1988) Investigation of large-scale circulation patterns in the central North Atlantic: The North Atlantic Current, the Azores Current and the Mediterranean Water plume in the area of the Mid-Atlantic Ridge. *Deep-Sea Research*, **35**, 383-413.
- SY, A., U. Schauer and J. Meincke (1992) The North Atlantic Current and its associated hydrographic structure above and eastwards of the Mid-Atlantic Ridge. *Deep-Sea Research*, **39**, 825-853.
- TALLEY, L.D. and M.S. MCCARTNEY (1982) Distribution and circulation of Labrador Sea water. *Journal of Physical Oceanography*, **12**, 1189-1205.
- TALLEY, L.D. and M.E. RAYMER (1982) Eighteen Degree Water variability. *Journal of Marine Research*, **40** (Supplement), 757-775.
- TOMCZAK, M. and P. HUGHES (1980) Three dimensional variability of water masses and currents in the Canary Current upwelling region. "Meteor" *Forschungs-Ergebnisse*, **A21**, 1-24.
- TUCHOLKE, B.E., W.R. WRIGHT and C.D. HOLLISTER (1973) Abyssal circulation over the Greater Antilles Outer Ridge. *Deep-Sea Research*, **20**, 973-995.
- WEATHERLY, G.L. and E.A. KELLY (1985) Two views of the cold filament. *Journal of Physical Oceanography*, **15**, 68-81.
- WESSEL, P. and W.H.F. SMITH (1991) Free software helps map and display data. *EOS Transactions, AGU*, **72**, 445-446.
- WORTHINGTON, L.V. (1954) Three detailed cross-sections of the Gulf Stream. *Tellus*, **6**, 116-123.
- WORTHINGTON, L.V. (1959) The 18° water in the Sargasso Sea. *Deep-Sea Research*, **5**, 297-305.
- WORTHINGTON, L.V. (1970) The Norwegian Sea as a Mediterranean basin. *Deep-Sea Research*, **17**, 77-84.
- WORTHINGTON, L.V. (1976) *On the North Atlantic Circulation*. The Johns Hopkins Oceanographic Studies, **6**, 110pp.
- WORTHINGTON, L.V. and W.R. WRIGHT (1970) North Atlantic Ocean Atlas of potential temperature and salinity in the deep water including temperature, salinity, and oxygen profiles from the Erika Dan cruise of 1962. Woods Hole Oceanographic Institution Atlas Series, **2**, 24pp and 58 plates.
- WRIGHT, W.R. and L.V. WORTHINGTON (1970) The water masses of the North Atlantic Ocean. A volumetric census of temperature and salinity. *Serial Atlas of the Marine Environment*, Folio **19**, American Geographic Society, 88pp and 7 plates.
- WÜST, G. and A. DE FANT (1936) Atlas zur Schichtung und Zirkulation des Atlantischen Ozeans. Schnitte und Karten von Temperatur, Salzgehalt und Dichte. In: *Wissenschaftliche Ergebnisse der Deutschen Atlantischen Expedition auf dem Forschungs- und Vermessungsschiff "Meteor" 1925-1927*, **6**, Atlas, 103 plates.
- ZHANG, H.-M. and N.G. HOGG (1992) Circulation and water mass balance in the Brazil Basin. *Journal of Marine Research*, **50**, 385-420.